Time series analysis based on paleoclimatic proxies from lake sediments in Iceland

Kristín Björg Ólafsdóttir

Faculty of Earth Sciences
University of Iceland
2010

Time series analysis based on paleoclimatic proxies from lake sediments in Iceland

Kristín Björg Ólafsdóttir

90 ECTS thesis submitted in partial fulfillment of a
Magister Scientiarum degree in Geology

Advisors
Áslaug Geirsdóttir
Ólafur Pétur Pálsson
Gifford H. Miller

Faculty Representative
Tómas Jóhannesson

Faculty of Earth Sciences
School of Engineering and Natural Sciences
University of Iceland
Reykjavik, February 2010

Time series analysis based on paleoclimatic proxies from lake sediments in Iceland

90 ECTS thesis submitted in partial fulfillment of a *Magister Scientiarum* degree in Geology

Faculty of Earth Sciences
School of Engineering and Natural Sciences
University of Iceland
Askja, Sturlugata 7
107, Reykjavik
Iceland

Telephone: 525 4000

Bibliographic information:
Kristín Björg Ólafsdóttir, 2010, *Time series analyses based on paleoclimatic proxies from lake sediments in Iceland*, Master's thesis, Faculty of Earth Sciences, University of Iceland, pp. 77.

ISBN XX

Printing: Háskólaprent ehf.
Reykjavik, Iceland, February 2010

Abstract

High-resolution proxy data that can be used to reconstruct temperature variability through time is essential in order to estimate the amplification of present warming compared with previous times. This thesis presents results from statistical analyses of paleoclimate records from sedimentary cores recovered from two different lakes in Iceland. The aim of the research was to determine if these proxy records preserve regular climate periodicities and whether the periodicities can be explained by external forces that have influenced past environmental changes in the North Atlantic region.

The first part discusses proxy data from lake sediments spanning the past 10,000 years recovered from Haukadalsvatn, a lake in northwestern Iceland. The spectral analyses of the proxies, biogenic silica (BSi) and total organic carbon (TOC), indicate significant periodicities through the last 10 ka. In the BSi record ~1200, 130, 90 and 70 year cycles are most apparent, whereas ~220, 47 and 40 year cycle are predominant in the TOC record. Differences in the periodicities of the two proxies are explained by differences in their primary controls. The periodicities in the BSi show considerably more stability through time than in the TOC record, where irregularity is due to competition between within-lake productivity and terrestrial soil erosion as the controlling variables on TOC. The climate proxies preserved in Haukadalsvatn‘s sediment is thought to respond to known climate variability in the North Atlantic tied to changes in both oceanic and atmospheric variability.

In the second part, a 3000-year varve-thickness record from Hvítárvatn, a glacial lake in central Iceland was used. The first-order low-frequency trend of the varve thickness record reflects increased erosion through the Late Holocene, reaching a peak during the Little Ice Age (LIA). Superimposed on this trend are large inter-annual to decadal fluctuations in varve thickness. The spectral analyses show that dominant variations in the varve thickness record, after removing the non-linear low-frequency variability, are 100 to 85, 35, 13, 5 and 2 to 4 year cycles. Some of these cycles show similar variability to the North Atlantic Oscillation (NAO) and Atlantic Multidecadal Oscillation (AMO). That relationship is supported by a significant correlation between varve thickness and summer NAO index as well as summer AMO index in the time domain.

Útdráttur

Samanburður á beinum veðurfarsathugunum og upplýsingum sem fyrir liggja um fornloftslag benda til þess að mun hraðari hlýnun hafi átt sér stað á 20. öldinni í samanburði við síðustu þúsund ár. Til þess að meta stærð og áhrif slíkra hlýnunar er nauðsynlegt að skoða loftslagsháð gögn lengra aftur í tíma og með háa tímaupplausn. Þessar rannsóknir greina frá niðurstöðum tölfræðigreiningar á loftslagsháðum gögnum úr stöðuvatnaseti frá tveimur mismunandi stöðuvötnum á Íslandi. Markmið rannsóknarinnar er að athuga hvort gögnin endurspegli reglulegar veðurfarssveiflur og ef svo er, hvort um er að ræða þekktar sveiflur sem tengjast umhverfisbreytingum á Norður Atlantshafssvæðinu.

Í fyrri hlutanum eru skoðuð loftslagsháð gögn úr stöðuvatnaseti frá Haukadalsvatni í Dölum, sem spanna síðustu 10,000 árin. Tíðnigreining loftlagsháðu gagnanna, þ.e lífræns kísils og lífræns kolefnis, sýna marktækar reglubundnar sveiflur yfir síðustu 10,000 árin. Í lífræna kísilnum koma fram ~1200, 130, 90 og 70 ára sveiflur en ~220, 47 og 40 ára sveiflur eru ráðandi í lífræna kolefninu. Mismunandi sveiflur í breytunum tveimur má útskýra með ólíkum uppruna þeirra. Sveiflurnar í lífræna kísilnum eru mun stöðugri á þeim 10,000 árum sem til athugunar eru en sveiflur í lífræna kolefninu. Kolefnið á sér tvennskonar uppruna, annars vegar kolefni sem tengja má frumframleiðni í vatninu og hins vegar kolefni af landrænum uppruna sem berst til vatnsins með rofi. Loftslagsháðar sveiflur í seti Haukadalsvatns eru taldar fylgja veðurfarsbreytingum í Norður Atlantshafi sem eru tengdar breytileika í sjávarstraumum og ráðandi loftmössum.

Hins vegar er 3000 ára ferill hvarflagaþykktar frá Hvítávatni, við Langjökul á miðhálendi Íslands, skoðaður. Langtímaleitni í ferli hvarflagaþykktarinnar sýnir aukið rof á seinnihluta nútíma, sem nær hámarki á Litlu ísöldinni (u.þ.b. 1400-1900 AD). Auk langtímaleitninnar í ferli hvarflagaþykktarinnar má finna minni sveiflur á árs- til áratugakvarða. Niðurstöður tíðnigreiningar sýna 100 til 85, 35, 13, 5 og 2 til 4 ára sveiflur í hvarflagaþykkt eftir að langtímaleitnin hefur verið dregin frá. Sumar þessara sveiflna eru svipaðar og finnast í Norður Atlantshafssveiflunni (NAO) og tengdum fyrirbrigðunum (AMO). Sambandið þar á milli er staðfest með marktækri fylgni á milli hvarflagaþykktar Hvítárvatns og sumarbreytileika fyrirbrigðanna tveggja (NAO og AMO) í tímarúmi.

Table of Contents

List of Figures ..... **ix**

List of Tables ..... **xi**

Acknowledgements ..... **xiii**

Chapter 1 ..... **1**

Introduction **1**
1 The purpose of the Study 1
2 The Study areas 4
2.1 Haukadalsvatn 4
2.2 Hvítárvatn 5
3 Proxies used 6
3.1 Biogenic silica and total organic carbon 6
3.2 Varve thickness 8
4 Methods 8
4.1 Spectral Analysis 8
4.2 Singular Spectrum Analysis 9
4.3 Multi Taper Method 10
4.4 Wavelet analysis 10
5 Results Summary 11
5.1 Paper 1 11
Periodicities in Holocene lacustrine paleoclimate proxies from Haukadalsvatn, Iceland 11
5.2 Paper 2 11
Climate inferences from high-frequency cyclicity in a 3-ka varve-thickness record from Hvítárvatn, Iceland 11
6 Future work 12
References 13

Chapter 2 ..... **15**

Periodicities in Holocene lacustrine paleoclimate proxies from Haukadalsvatn, Iceland **15**
1 Introduction 16
1.1 Objectives 16
1.2 Background 17
2 Materials 20
2.1 Regional Setting 20
2.2 The sediment cores from Haukadalsvatn 21
2.3 Chronology 21
2.4 Biogenic silica and total organic carbon variables 22

3 Data Analysis 22
3.1 Data processing 22
3.2 Spectral Analysis 23
4 Results 26
4.1 Low frequency trend in the BSi and TOC records 26
4.2 Cyclicity in the BSi record 26
4.3 Cyclicity in the TOC record 28
5 Discussion 29
5.1 Centennial and decadal variability in the BSi and TOC variables 29
5.2 The mechanism of the periodicities 30
6 Conclusion 33

Chapter 3 51

Climate inferences from high-frequency cyclicity in a 3-ka varve-thickness record from Hvítárvatn, Iceland 51
1 Introduction 52
2 Regional setting 54
3 Materials and methods: 54
4 Results 56
4.1 The long term variation in the varve thickness record 56
4.2 High-frequency cyclicity on annual to decadal time scales 56
5 Discussion 58
5.1 Long-term changes in glacier extent 58
5.2 Understanding controls on high-frequency variations in varve thickness: a summer climate proxy 58
5.3 Correlation with the North Atlantic Oscillation 60
5.4 Evolution of cyclicities over the past 3 ka 62
6 Conclusion 63

List of Figures

Chapter 1:

Introduction

Figure 1 *Sea surface currents around Iceland and Geological map of Iceland.* 2

Figure 2 *Haukadalsvatn* 5

Figure 3 *Hvítárvatn* 6

Figure 4 *Biogenic Silica compared with instrumental climate data from Stykkishólmur.* 7

Figure 5 *Total organic carbon compared with wind speeds during the winter months recorded nearby Stykkishólmur weather station.* 7

Figure 6 *Varve thickness from Hvítárvatn sediment core.* 8

Chapter 2:

Periodicities in Holocene lacustrine paleoclimate proxies from Haukadalsvatn, Iceland

Figure 1 *Geographical information of Iceland and Haukadalsvatn* 41

Figure 2 *The age model for the sediment core from Haukadalsvatn* 41

Figure 3 *The raw and detrended record of Biogenic Silica (BSi) from the sediment core from Haukadalsvatn* 42

Figure 4 *The raw and detrended record of Total Organic Carbon (TOC) from the sediment core from Haukadalsvatn* 43

Figure 5 *Spectral Analysis for the BSi record from the sediment core from Haukadalsvatn* 44

Figure 6 *Wavelet power spectrum of the BSi record from Haukadalsvatn and reconstructed components from the SSA spectrum for the BSi records as a function of time* 45

Figure 7 *The main cycles (1200, 130, 90 and 70) in the BSi record recontructed and plotted up as a function of time* 46

Figure 8 *Spectral Analysis for the TOC record in the core from Haukadalsvatn.* 47

Figure 9 *Wavelet power spectrum for the TOC record from Haukadalsvatn and reconstructed components from the SSA spectrum for the TOC records as a function of time.* 48

Figure 10 *The main cycles (~220, 47 and 40 year cycles) in the TOC record reconstructed and plotted up as a function of time* 49

Chapter 3:

Climate inferences from high-frequency cyclicity in a 3-ka varve-thickness record from Hvítárvatn Iceland

Figure 1 *Langjökull and location of Hvítárvatn and the meteorological stations at Hveravellir and Stykkishólmur* 67

Figure 2 *Topographic map of Hvítárvatn and Langjökull.* 68

Figure 3 *The raw and detrended record of varve thickness from Hvítárvatn* 69

Figure 4 *Spectral analyses for the varve thickness record from Hvítárvatn* 70

Figure 5 *Wavelet power spectrum of the varve thickness record from Hvítárvatn* 71

Figure 6 *Instrumental climate records from Stykkishólmur and Hveravellir* 72

Figure 7 *Comparison between the varve thickness from Hvítárvatn and composite record of climate parameters from Stykkishólmur and Hveravellir* 73

Figure 8 *Comparison of the varve thickness record from Hvítarvatn, summer AMO index, summer NAO index, summer temperature and summer precipitation* 74

Figure 9 *Spectral analyses of the varve thickness recrod from Hvítárvatn, splitted up into two segments; the Neoglciation part (1250 AD -830 BP) and the Little Ice Age part (2002-1250 AD)* 75

List of Tables

Chapter 2:

Periodicities in Holocene lacustrine paleoclimate proxies from Haukadalsvatn, Iceland

Table 1 *List of significant periods from the Biogenic Silica (BSi) and Total Organic Carbon (TOC) indicated with the SSA,MTM and the wavelet power spectrum.*..... 50

Chapter 3:

Climate inferences from high-frequency cyclicity in a 3-ka varve-thickness record from Hvítárvatn Iceland

Table 1 *Table of correlation between the varve thickness from Hvítárvatn and composite records of temperature and precipitation from from Hveravellir (2002 -1966 AD) and Stykkishólmur (1965 – 1830 AD)*..... 76

Table 2 *Table of correlation between the varve thickness and NAO and AMO summer indices* 77

Acknowledgements

First of all I would like to thank my main supervisor Áslaug Geirsdóttir for continuous support and encouragement. For introducing me to this field of study and for expanding my knowledge and interest by including the time series analysis into my project. I want to thank Gifford H. Miller for all the inspiring help by keep asking more and more challenging questions and for improving the English in the articles. I want to thank Ólafur Pétur Pálsson for all the help with the statistics during my work.

Financial support for this project was received from The Research Fund of the University of Iceland to Áslaug Geirsdóttir, The Environmental and Energy Research Fund from the Reykjavik Energy, The Icelandic Centre for Research - RANNÍS (Áslaug Geirsdóttir contract nr #0070272011) in addition to a one year M.Sc. Grant from the Icelandic Research Fund for Graduate Students.

I want to thank Trausti Jónsson, at the Icelandic Meteorological Office, for donating the extended temperature- and precipitation- records from Stykkishólmur. I would like to thank Darren Larsen for letting me use his varve data and for reading a draft of my article. I am grateful to the people at INSTAAR for warm and stimulating atmosphere during my visit there. John Andrews is thanked for recommending the time series computer programs and for the beginner help to learn how to use them. I want to thank my office mate and fellow student Sædís Ólafsdóttir for endless support through the years and for being such a good friend. In addition I want to thank fellow students and co-workers at Askja for inspiring support and good company. Finally I like to thank my boyfriend and my family for encouraging me and being always there for me when needed.

Chapter 1

Introduction

This Master thesis is based on the following article manuscripts that are planned to be submitted in a peer-reviewed international journal. The manuscripts are included as chapters 2 and 3:

- *Periodicities in Holocene lacustrine paleoclimate proxies from Haukadalsvatn, Iceland.*
- *Climate inferences from high-frequency cyclicity in a 3-ka varve-thickness record from Hvítárvatn, Iceland.*

1 The purpose of the Study

During the past century, global surface temperatures have increased by ~0.8°C, with even greater warming occurring at northern latitudes (IPCC, 2007). Climate models predict that the Arctic will warm by more than twice the global average in the next 100 years. It is generally accepted that increasing concentration of anthropogenic greenhouses gases in the atmosphere explains at least part of this warming (IPCC, 2007), although it is still unclear how much is caused by increased anthropogenic greenhouse gases and how much by natural variability. Therefore, interest has been growing to analyze high-frequency climate variances in Holocene paleoclimate records that span longer time than the historical and instrumental records. Reconstructing climate cycles in the recent past is essential to constrain the magnitudes and rates of natural climate variability in the past and to evaluate the mechanisms that have caused environmental changes in the past. Iceland is an ideal region for studying variability in ocean currents and atmospheric dynamics. The island is located at the boundary between the relatively warm and saline Irminger Current, a branch of the North Atlantic Current originating in the tropics, and colder and low salinity East Greenland Current from the Arctic Ocean (Figure 1a). In addition, the climate in Iceland is sensitive to changes in storm tracks across the North Atlantic Ocean. Several studies have focused on periodicities in Holocene paleoclimate data from the North Shelf of Iceland (Andrews et al., 2003a and b, Rousse et al., 2006, Sicre et al., 2008a and b). However

there are no extensive studies of possible periodicities in terrestrial proxy data from Iceland. Such studies could give further information how the natural climate variablitiy controlled the climate system in Iceland in the past and whether the forcing mechanisms have shown a stable behaviour through the time.

The primary goal of this Master‘s thesis is to use available lake sediment cores from two different lakes in Iceland, that contain paleoclimatic proxy data, to analyse whether regular patterns of centennial and higher frequencies exist in the proxies. In paper 1 the study area is the non-glacial lake Haukadalsvatn, a low-lying coastal lake in northwestern Iceland (Figure 1b). The study area in Paper 2 is the glacial lake Hvítárvatn, located on the eastern margin of Langjökull up in the highland in central Iceland (Figure 1b). This research should give new information on the pattern of climate behavior in Iceland back in time, as it is reflected in the proxy records. From the proxy data from Haukadalsvatn it is possible to analyze longer term changes in the system over a ~10.000 year period whereas from the Hvítárvatn data it is possible to analyze much higher frequency changes in the lake system over the past ~3000 years. The data used and the research goals are listed below.

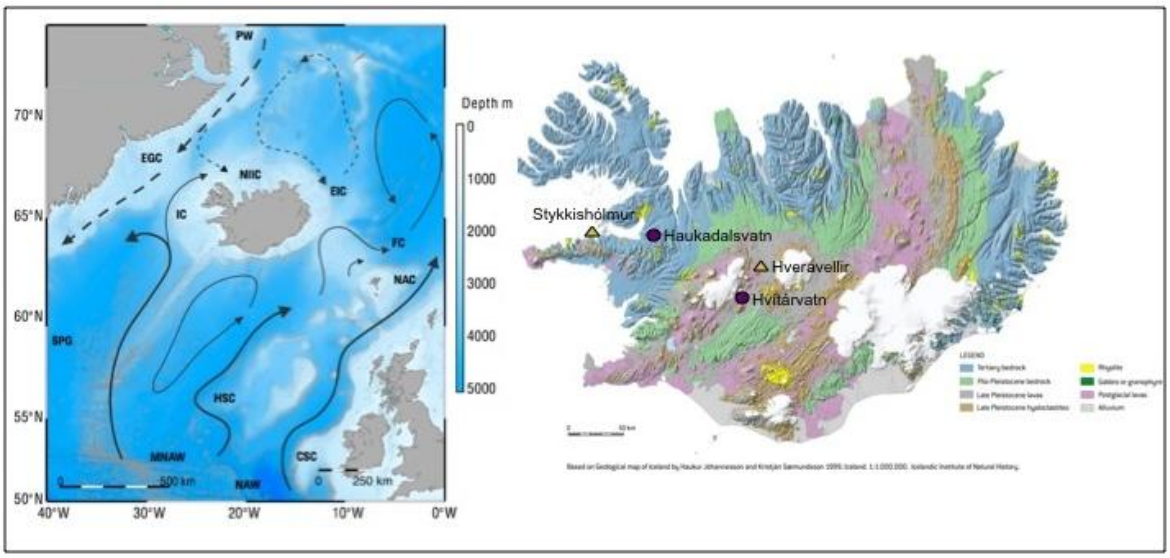

Figure 1 ***a)*** *Sea surface currents around Iceland. PW=Polar water, EGC=East Greenland Current, EIC=East Iceland Current, IC=Irminger Current, SPG=Subpolar Gyre, HSC=Hatton Slope Current, CSC=Continental Slope Current, NAC=North Atlantic Current, FC=Faroe Current (modified from Hansen and Østerhus, 2000).* ***b)****. Geological map of Iceland. Study sites are marked with red circles, Hvítárvatn and Haukadalsvatn. Instrumental weather data from Stykkishólmur and Hveravellir are used in this study.*

Paper 1 – Haukadalsvatn:

- Data:
  - Paleoclimate proxies: Biogenic Silica (BSi) and Total Organic Carbon (TOC) from a sediment core from Haukadalsvatn.
  - Chronology based on known tephra layers throughout the core.
- Time interval:
  - The past 10,200 years.
- Sampling intervals:
  - Bidecadal resolution.
- Research aims and questions:
  - Apply statistical analyses to determine whether the climate proxies have periodicities at decadal to centennial time-scales?
  - Do the cycles change over the Holocene?
  - Do the two climate proxies have coherent periodicities and if so, is it possible to extract information of the controls of the periodicities?
  - Is there a correlation between the Haukadalsvatn proxies with known cycles explained by external forces that have influenced environmental changes in this region?

Paper 2 – Hvítárvatn:

- Data:
  - Paleoclimate proxies: Varve thickness record from Hvítárvatn.
  - Chronology based on varve counting constrained by known tephra layers.
- Time interval:
  - The past ~3000 years.
- Sampling intervals:
  - Annual resolution.
- Research aims and questions:
  - To test whether inter-annual to decadal periodicities are superimposed on a long-term trend in the varve-thickness record, which is interpreted to be a proxy for glacial erosive power.

- To test for correlation between varve thickness and specific climate parameters brought from nearby weather stations.
- Spectral analyses are used to test whether high-frequency variations in the varve record show any regular periodicities.
- To analyze whether the indicated cycles change over time?
- To evaluate possible connections to known climatic variability.

2 The Study areas

2.1 Haukadalsvatn

Lake Haukadalsvatn is a glacier-eroded lake at the head of Hvammsfjörður, western Iceland (Fig. 2). The 40-m-deep lake has a surface area of 3,28 km^2 and a catchment of 172 km^2, mostly above 500m asl. The lake acts as sediment trap resulting in sedimentation rates that exceed 1.5 m/ka in the central basin. The surrounding bedrock is Tertiary basalt and the region lies outside the extant volcanic zones of Iceland (Jóhannesson, 1997). The valley of Haukadalur was depressed during glaciations (postglacial marine limit ~70m asl) and the earliest sediment fill in Haukadalsvatn is of marine origin, before isostatic recovery elevated the valley above sea level about 10.6 ka ago (Geirsdóttir et al., 2009b). The soils around Haukadalsvatn are mostly andosols (eolian and tephra) but histosols can also been found near the lake (Arnalds and Grétarsson, 2001). Andosols are porous and have a tendency to bind organic matter that makes it fertile. On the other hand this type of soil often lacks cohesion that makes it vulnerable to disturbance that can cause landslides and erosion by wind and water (Arnalds, 2004). Historical accounts describe the valley of Haukadalur as being heavily forested at the time of settlement; today there is no forest in the valley but it is vegetated by grasses and sedges. The Haukadalur valley has been inhabited since the 10^{th} century.

Figure 2 *Haukadalsvatn in Haukadalur looking towards the highlands in the east.*

2.2 Hvítárvatn

Hvítárvatn (elev. 421m asl, area 28.9 km^2, max. depth 83 m) is located on the eastern margin of Langjökull, Iceland's second largest ice cap (Fig. 3). Runoff to the lake is dominated by melt water from Langjökull; in addition, two outlet glaciers, Norðurjökull and Suðurjökull, terminated in the lake during the Little Ice Age (LIA; see Fig.2 in Chapter 3). Norðurjökull has been calving into the lake since the LIA, whereas Suðurjökull retreated from the lake around 1950 AD. Fluctuations in the two outlet glaciers reflect climate change, as they are not known to be surging glaciers and there has not been active volcanism affecting this portion of Langjökull during past 3 ka. The varve thicknesses record the sediment flux to the lake, which is dominated by changes in the erosive power of Langjökull, modulated by shorter-term fluctuations in the efficiency of the subglacial hydrologic system to deliver the eroded sediment to the lake.

Figure 3 *Hvítárvatn by Langjökull.*

3 Proxies used

3.1 Biogenic silica and total organic carbon

In paper 1, two climate proxies are used from the sediment core from Haukadalsvatn, Biogenic Silica (BSi) and Total Organic Carbon (TOC). They are measured every 1-10 cm for the past 10.2 ka with the highest resolution in the uppermost part of the core. This provides a 1-5 year resolution for the past 2ka, and decadal resolution between 10 and 2 ka.

Geirsdóttir et al. (2009a) argue that BSi in Haukadalsvatn is a proxy for aquatic primary productivity, which reflects warm April-May temperatures. This is based on a fairly strong correlation between the BSi record with 170-year long instrumental spring temperature record (April – May) from Stykkishólmur, a weather station close to Haukadalsvatn (Figure 4).

TOC peaks during the last 2000 years are shown to represent an increased flux of terrestrial carbon to the lake from eolian-derived soil erosion following periods of cold summers accompanied by dry, windy winters (Geirsdóttir et al., 2009a). The interpretation is based on a strong correlation between measured high values of TOC and C:N and $\delta^{13}C$ peaks that reflect a greater proportion of terrestrial carbon. The role of wind is based on a

positive correlation between TOC peaks and wind strength record from the Stykkishólmur weather station (Fig 5 ; Geirsdóttir et al., 2009a).

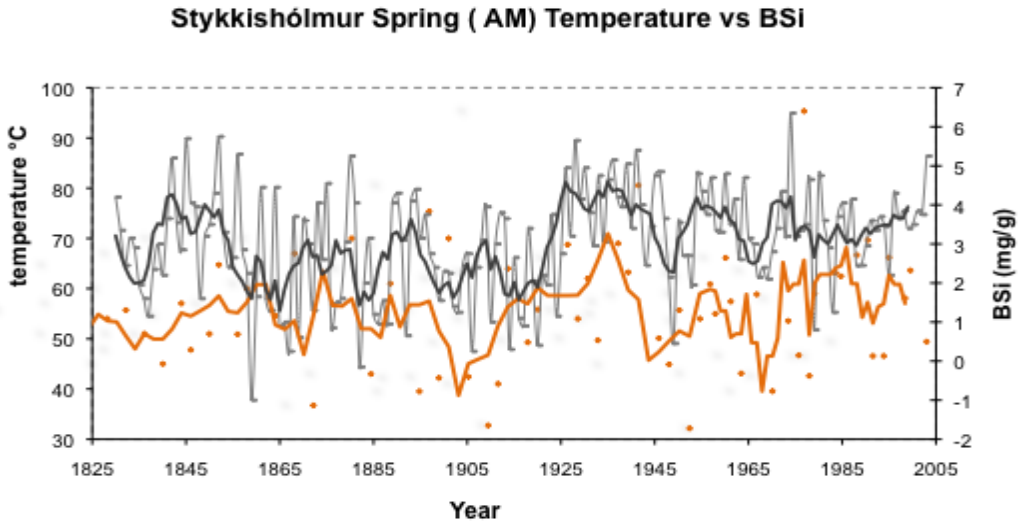

Figure 4 *Biogenic Silica (BSi) content compared with instrumental data from Stykkishólmur, April-May (AM) temperature. BSi (orange line) and temperature (gray line). Bold lines show 5-year running means.*

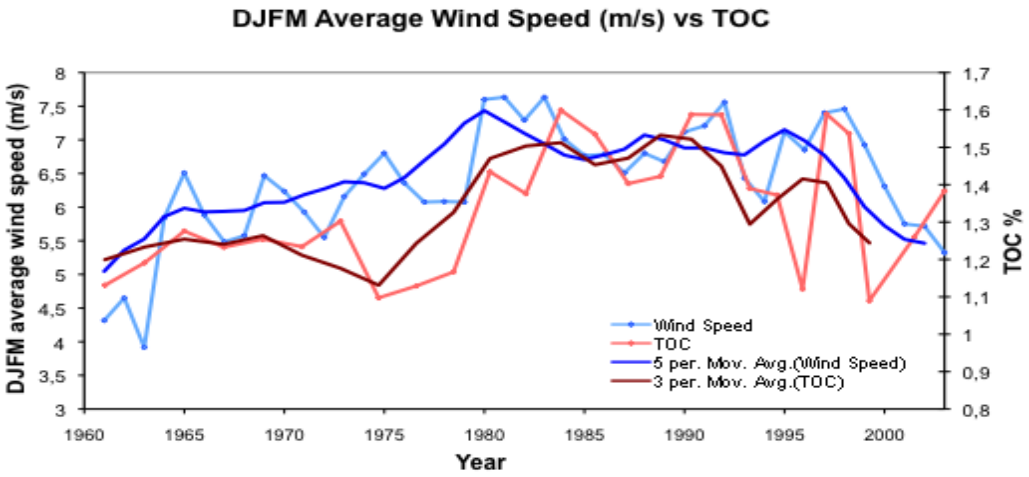

Figure 5 *Total organic carbon (TOC) content from HAK03-1B (red) compared with mean monthly wind speeds (circles) during the winter months (DJFM) recorded nearby Stykkishólmur weather station. Wind speed records are only available from 1964 (www.vedur.is). Bold curves are 5-year moving averages.*

3.2 Varve thickness

In paper 2, a varve thickness record from a sedimentary core from Hvítárvatn (Figure 6), is used as a climate proxy. The thickness of each annual lamina (varve) from this core represents the annual sediment flux to the lake. Varves have been counted and varve thicknesses measured for the past 3000 years of sedimentation (Figure 6; Larsen et al., in prep.). The first-order trend of the varve thickness record is believed to reflect changes in the amount of glacial erosion occurring in the lake's catchment, which is a proxy for the size of Langjökull. The objective in the paper was to explore the potential climate significance of the higher frequency signal in the varve-thickness record. Tephrochronology and cross-correlation techniques on distinctive tephra and laminae patterns of four sediment cores taken from the northern basin of Hvítárvatn confirms the annual nature of the laminae in the lakes (Larsen et al., in prep.).

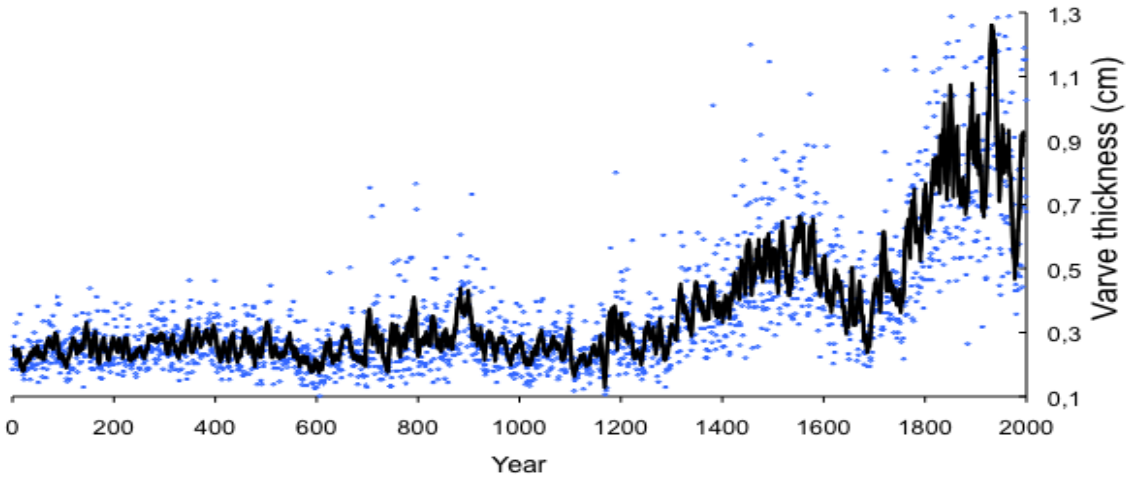

Figure 6 *Varve thickness from Hvítárvatn sediment core. Solid lines represent 20 year moving averages*

4 Methods

4.1 Spectral Analysis

Time series analyses are used to identify the nature of the phenomenon represented by the sequence of observations and to predict future values of the time series variable (Ghil et al., 2002). Spectral analyses are widely used to detect periodic or quasi periodic components in time series, which are indicated by peaks that can be distinguished from background noise (Weedon, 2003). The classic method for estimating a spectral density is

the periodogram that is formed by taking the Fourier transform of the autocovariance function of the time series. Now more advanced methods have appeared where the goal is to reduce spectral bias, variances and leakage of the spectral plot, to increase accuracy as well as adding new and more advanced features. In the following papers Singular Spectrum Analysis (SSA) (Vautard and Ghil, 1989) and Multi Taper Method (MTM) (Thomson, 1982) in the kSpectra 2.13 Toolkit (http://www.spectraworks.com) were both used to identify the significant periodicities in the time series. In addition, the interactive wavelet analysis toolkit on http://paos.colorado.edu/research/wavelets/ (Torrence and Compo, 1998) was used to analyze how the spectral power varies over the time.

4.2 Singular Spectrum Analysis

Singular Spectrum Analysis (SSA) is one of many spectral analyse methods that is suitable for decomposing short, noisy signals into a (nonlinear) trend, oscillatory components and noise (Ghil et al., 2002). The first step is to embed the time series into phase space of M dimensions. After that, the data are treated as a series of variables, one for each embedding dimension, and a matrix is formed of the variance and covariance for every dimension being considered. The covariance matrix is diagonalized and the eigenvalues are ranked in decreasing order but the eigenvalue gives the variance of the time series in the direction specified by the corresponding eigenvector. The square root of the eigenvalues gives the singular values, which are plotted up in decreasing order to form a singular spectrum (Vautard and Ghil, 1989). The singular spectrum is used to separate signal from noise by defining components with the most variance significantly larger than other components that are identified as noise. This method works well if the noise is likely to be white noise, but in climatic and geophysical time series the noise is usually red noise which tends to have larger power at lower frequencies. Then it is necessary to use significance tests such as Monte Carlo SSA (Allen and Smith, 1996), which tests significance against a red-noise hypothesis. The eigenvalues and eigenvectors define empirical orthogonal function (EOFs) in phase space. It is possible to project the time series onto each EOF to get the corresponding principal components that can be plotted up as reconstructed components (RCs) in time space, which preserve amplitude, frequency and phase of the time series (Vautard and Ghil, 1989).

4.3 Multi Taper Method

Multi Taper method (MTM) is used to reduce the variance of spectral estimates by using a small set of tapers (Thomson, 1982). These tapers are known as discrete prolate spheroidal sequences or Slepian sequences and are constructed to minimize the spectral leakage due to the finite length of the time series. The purpose of the MTM is to produce a power spectrum with small bias, good smoothing and yet high frequency resolution. A number of tapers are chosen according to the data analyzed depending on the length of the data sets and other properties of the time series. The choice of bandwidth and number of tapers reflects the classical trade off between spectral resolution and the stability of the spectral estimate (Thomson, 1982). A set of independent estimates of the power spectrum is computed by pre-multiplying the data by each orthogonal taper and then the total power spectrum is computed by averaging all the individual spectra. The peaks that appear in the power spectrum are tested for significance relative to the null hypothesis of a red-noise background estimated from the data (Mann and Lees, 1996). Confidence levels relative to the estimated red-noise background can be determined from the appropriate quantiles of the chi-squared distribution.

4.4 Wavelet analysis

Wavelet analyses are used to analyze how periodicities change over time and are applicable to time series that do not contain stationary power at definite frequencies. The time series is decomposed into time-frequency space by using a wavelet, an orthogonal function where the oscillations die away to zero rather than going on indefinitely. An appropriate mother wavelet function is chosen, that can be stretched and translated with flexible resolution in both frequency and time space, and multiplied with the times series to produce a wavelet transform (Torrence and Compo, 1998). Background spectrum is chosen either red or white noise and the peaks in the wavelet power spectrum above this background spectrum are assumed to be real feature.

5 Results Summary

5.1 Paper 1

Periodicities in Holocene lacustrine paleoclimate proxies from Haukadalsvatn, Iceland

A thick sequence of lake sediments recovered from Haukadalsvatn, a lake in northwestern Iceland, contains paleoclimatic proxy data at high resolution spanning the past 10,000 years. These proxy records were used to determine whether the sediment preserves regular decadal to centennial climate periodicities. The spectral analysis of the proxies, biogenic silica (BSi), and total organic carbon (TOC), indicates significant periodicities through the last 10 ka, although the BSi and TOC time series do not show the same primary cycles. In the BSi record ~1200, 130, 90 and 70 year cycles are most apparent, whereas ~220, 47 and 40 year cycle are predominant in the TOC record. Differences in the periodicities of the two proxies may be explained by differences in their primary controls. The periodicities in the BSi show considerably more stability through time than in the TOC record, where irregularity is due to competition between within-lake productivity and terrestrial soil erosion as the controlling variables on TOC. We hypothesize that the main forcing of the most prominent cycles in both BSi and TOC records from HAK is related to the Atlantic Multidecadal Oscillation (AMO) and North Atlantic Oscillation (NAO). In addition some of the cycles show similiarities to known solar cycles.

5.2 Paper 2

Climate inferences from high-frequency cyclicity in a 3-ka varve-thickness record from Hvítárvatn, Iceland

A 3000-year varve-thickness record from Hvítárvatn, a glacial lake in central Iceland, preserves inter-annual variations in the delivery of glacially-eroded sediment to the lake. The first-order low-frequency trend of the varve thickness record reflects increased erosion through the Late Holocene, reaching a peak during the Little Ice Age (LIA). Superimposed on this trend are large inter-annual to decadal fluctuations in varve thickness that we suggest reflect variability in climate parameters that influence the amount of eroded sediment that is delivered to the lake each year. Here we use spectral analysis to test whether regular high-frequency cyclicity in varve thickness exists in the 3 ka varve thickness record from Hvítárvatn after removing the non-linear low-frequency variability. The spectral analyses show that dominant variations in the varve thickness record are 100

to 85, 35, 13, 5 and 2 to 4 year cycles. Some of these cycles show similar variability to that of the North Atlantic Oscillation (NAO) and Atlantic Multidecadal Oscillation (AMO). That relationship is supported by a significant correlation between varve thickness and summer NAO index as well as summer AMO index in the time domain. Comparison of the past 800 years, during which varve thicknesses are greater and more variable, with the earlier and more stable part, demonstrates that most of the dominant cycles are continuous through the entire 3ka record, both before and during the Little Ice Age. However, cycles similar to known solar cycles that appear in the early part of the record, are not detected in the Little Ice Age (LIA, ca. 1200-1900 AD) portion of the time series, suggesting that a higher frequency solar variability played a minor role in climate forcing variability during the LIA.

6 Future work

A future work could focus on the last 2000 years of the proxy data from Haukadalsvatn. Data with much higher resolution are available from this part of the sediment core where the resolution is 1 – 5 years whereas the data has a bidecadal resolution in Paper 1. It would be interesting to study whether new cycles of higher frequency would appear in the more recent part and whether some of the longer term cycles in paper 1 are product of aliasing of higher frequency cycles. It would also give an opportunity to compare the results with the obtained cycles in the varve thickness results from Hvítárvatn, discussed in Paper 2. In the present study there is too much difference in the time resolution for direct comparison. It would be interesting to see whether there are differences in the mechanism(s) influencing a low lying coastal lake and a glacier lake up in the highland. Do the solar forces have more influences on the lake in the inland than on the coastal lake?

It would also be patent to use a cross spectral analysis in addition to the methods used in the present research. Cross spectral analysis is used to find coherent periodicities between two time series. It would be ideal to find coherent cycles between the two proxies in the HAK record and to analyze further the correlation between the varve thickness and climate indices like NAO and AMO.

References

Allen, M. R., and Smith, L. A. (1996). Monte Carlo SSA: Detecting irregular oscillations in the presence of colored noise. *Journal of Climate* **9,** 3373-3404.

Andrews, J. T., Harðardóttir, J., Kristjánsdóttir, G. B., Grönvold, K., and Stoner, J. S. (2003a). A high-resolution Holocene sediment record from Húnaflóaáll, N Iceland margin: century- to millennial-scale variability since the Vedde tephra. *The Holocene* **13,** 625-638.

Andrews, J. T., Harðardóttir, J., Stoner, J. S., Mann, M. E., Kristjánsdóttir, G. B., and Koc, N. (2003b). Decadal to millennial-scale periodicities in North Iceland shelf sediments over the last 12000 cal yr: long -term North Atlantic oceanographic variability and solar forcing. *Earth and Planetary Science Letters* **210,** 453-465.

Arnalds, Ó. (2004). Volcanic soils of Iceland. *Catena* **56,** 3-20.

Arnalds, Ó., and Grétarsson, E. (2001). Soil Map of Iceland. Agriculture Research Institute, Reykjavík.

Geirsdóttir, Á., Miller, G., H., Thordarson, T., and Ólafsdóttir, K., B. (2009a). A 2000 year record of climate variations reconstructed from Haukadalsvatn, West Iceland. *Journal of Paleolimnology* **41,** 95-115.

Geirsdóttir, Á., Miller, G. H., Axford, Y., and Ólafsdóttir, S. (2009b). Holocene and latest Pleistocene climate and glacier fluctuations in Iceland. *Quaternary Science Reviews* **28,** 2107-2118.

Ghil, M., Allen, M. R., Dettinger, M. D., Ide, K., Kondrashov, D., Mann, M. E., Robertson, A. W., Saunders, A., Tian, Y., Varadi, F., and Yiou, P. (2002). Advanced spectral methods for climatic time series. *Reviews of Geophysics* **40,** 1-41.

Hansen, B., and Osterhus, S. (2000). North Atlantic-Nordic Seas exchanges. *Progress in Oceanography* **42,** 109-208.

IPCC. (2007). Intergovernmental Panel on Climate Change (IPCC) Fourth Assessment Report - Climate Change 2007. Summary for Policymakers.

Jóhannesson, H. (1997). Yfirlit um jarðfræði hálendis Mýrasýslu og yfir til Dala. *In* "Í fjallhögum milli Mýra og Dala Árbók Ferðafélag Íslands." (G. Á. Grímsdóttir, and Á. Björnsson, Eds.), pp. 215-226. Ferðafélag Íslands, Reykjavík.

Mann, M. E., and Lees, J. M. (1996). Robust estimation of background noise and signal detection in climatic time series. *Climatic Change* **33,** 409-445.

Rousse, S., Kissel, C., Laj, C., Eiríksson, J., and Knudsen, K.-L. (2006). Holocene centennial to millennial-scale climate variability: Evidence from high-resolution magnetic analysis of the last 10 cal kyr off North Iceland (core MD99-2275). *Earth and Planetary Science Letters* **242,** 390-405.

Sicre, M.-A., Jacob, J., Ezat, U., Rousse, S., Kissel, C., Yiou, P., Eiríksson, J., Knudsen, K. L., Jansen, E., and Turon, J.-L. (2008a). Decadal variability of sea surface temperatures off North Iceland over the last 2000 years. *Earth and Planetary Science Letters* **268,** 137-142.

Sicre, M.-A., Yiou, P., Eiríksson, J., Ezat, U., Guimbaut, E., Dahhaoui, I., Knudsen, K.-L., Jansen, E., and Turon, J.-L. (2008b). A 4500-year reconstruction of sea surface temperature variability at decadal time-scales off North Iceland. *Quaternary Science Reviews* **27,** 2041-2047.

Thomson, D. J. (1982). Spectrum estimation and harmonic analysis. *Proceedings of the IEEE* **70,** 1055-1096.

Torrence, C., and Compo, G. P. (1998). A practical guide to wavelet analysis. *Bulletin of the American Meteorological Society* **79,** 61-78.

Vautard, R., and Ghil, M. (1989). Singular spectrum analysis in non-linear dynamics, with application to paleoclimatic time series. *Physica D* **35,** 395-424.

Weedon, G. (2003). "Time-series analysis and cyclostratigraphy - Examining stratigraphic records of environmental cycles." Cambridge University Press, Cambridge.

Chapter 2

Periodicities in Holocene lacustrine paleoclimate proxies from Haukadalsvatn, Iceland

Kristín B. Ólafsdóttir, Áslaug Geirsdóttir, Ólafur P. Pálsson, Gifford H. Miller

Abstract

Decadal to centennial periodicities have been found in many Holocene paleoclimate proxies from the North Atlantic region. A thick sequence of lake sediments recovered from Haukadalsvatn, a lake in northwestern Iceland, contains paleoclimatic proxy data at high resolution spanning the past 10,000 years. These proxy records were used to determine whether the sediment preserves regular decadal to centennial climate periodicities. The spectral analysis of the proxies, biogenic silica (BSi), and total organic carbon (TOC), indicates significant periodicities through the last 10 ka, although the BSi and TOC time series do not show the same primary cycles. In the BSi record ~1200, 130, 90 and 70 year cycles are most apparent, whereas ~220, 47 and 40 year cycle are predominant in the TOC record. Differences in the periodicities of the two proxies may be explained by differences in their primary controls. The periodicities in the BSi show considerably more stability through time than in the TOC record, where irregularity is due to competition between within-lake productivity and terrestrial soil erosion as the controlling variables on TOC. We hypothesize that the main forcing of the most prominent cycles in both BSi and TOC records from HAK is related to the Atlantic Multidecadal Oscillation (AMO) and North Atlantic Oscillation (NAO). In addition some of the cycles show similiarities to known solar cycles.

1 Introduction

1.1 Objectives

During the past century, global surface temperatures have increased by ~0.8°C (IPCC, 2007), with the greatest warming occurring in the Arctic (Serreze and Francis, 2006). Warming has already resulted in significant changes in the Arctic environment, including reduced snow cover, rapidly retreating glaciers, warmer ocean temperatures, rising sea levels, and deepening of the active layer in permafrost. It is generally accepted that the increasing concentration of anthropogenic greenhouse gases in the atmosphere explains at least a part of this warming (IPCC, 2007), although it is still unclear how much is caused by increased anthropogenic greenhouse gases and how much by natural climate variations. Reconstructing decadal to centennial climate cycles in the recent past is required to constrain the magnitudes and rates of natural climate variability, to elucidate cycles of climate change that are longer than the historical records, and to evaluate the mechanisms that have caused environmental changes in the past. Many paleoclimate records show periodicities on long time-scales (millennial and longer) that have been attributed to changes in Earth's orbital parameters, or so called Milankovitch forcing (e.g. Weedon, 1993 and Hinnov, 2000). Those are changes in obliquity, precession and eccentricity that produce periodicities of 22, 41 and 100 ka cycle, which are important climatically because of seasonal and latitudinal distribution of solar radiation. Lately the focus has been on high resolution Holocene paleoclimate records that have cyclicities on much shorter time-scales (e.g. Bond et al.,1997, 2001, Hu et al., 2003, Rousse et al., 2006, Sicre et al., 2008a and b).

In order to obtain a better picture of the spatial pattern of centennial and higher frequency climate variability, a high-resolution lake sediment core from Haukadalsvatn in northwestern Iceland that contains paleoclimatic proxy data back 10.2 ka is used. Geirsdóttir et al. (2009a) showed that biogenic-silica content was correlated significantly with spring/early-summer temperature at the lake, and they used organic-matter content, along with other organic-matter-source indices, to interpret landscape instability. The aim here is to apply statistical analyses to determine whether the climate proxies have periodicities at decadal to centennial time-scales. And if so, do the cycles change over the Holocene? Do the climate proxies have any coherent periodicity and if so, is it possible to extract information of the controls of the periodicity? Is there correlation between the

Haukadalsvatn proxies with known cycles explained by external forces that have influenced environmental changes in this region?

1.2 Background

1.2.1 Climate forcing and known periodicities during the Holocene

The main external forces affecting low frequency changes in Holocene climate are the insolation changes tied to orbital irregularities. In the early Holocene, precessional changes led to positive summer insolation anomalies at all latitudes across the Northern Hemisphere (Bradley, 2003). For climate changes on shorter time-scales the main climate forcing through the Holocene are changes in solar irradiance and/or volcanic effects (Bradley, 2003). The retreating ice sheets from the last glacial maximum affected the climate in early Holocene, by influxes of melt water causing temporary abrupt climate changes (Alley et al., 1997). Anthropogenic forcing has dominated during the past century, and it is no longer possible to explain the recent temperature rise by natural forces alone (Crowley, 2000, Amman et al., 2007).

There is evidence that the Sun's output varies on multi-decadal time-scales and statistical studies have attempted to correlate weather with solar variation (e.g. Lean et al., 1995). Solar activity shows quasi-periodicity at several cycle lengths, and these same periodicities are found in paleoclimate records (Cooper et al., 2000, Bond et al., 2001, Andrews et al., 2003b, Hu et al., 2003). The number of sunspots is correlated with solar luminosity, and has been counted continuously since the 17th century. The 11-year sunspot cycle, the best defined solar cycle, has been measured by satellites during recent decades. Total solar irradiance is measured by satellites to vary by ~0.1 % over the 11-year sunspot cycle, with a maximum when there are many sunspots (Frölich and Lean, 2004). The ~22 year Hale cycle is also present; during each sunspot cycle the magnetic field of the Sun returns to the same state after two reversals forming a 22-year cycle.

Changes in the production rates of cosmogenic isotopes (^{14}C from tree rings and ^{10}Be from ice cores) are used as a proxy for solar irradiance changes over time. From these proxies, solar cycles of longer time-scales are known, like the 80-90 year Gleissberg cycle (e.g. Stuiver and Braziunas, 1993, Peristykh and Damon, 2003, Rogers et al., 2006) thought to be an amplitude modulation of the 11-year cycle and the ~200 year Suess/de Vries cycle (e.g. Stuiver and Braziunas, 1993, Wagner et al., 2001, Peristykh and Damon,

2003, Rogers et al., 2006). There is also a 2000-2400 year cycle that is apparent in several records (Sonett and Finney, 1990, Vasiliev and Dergachev, 2002). Although a number of studies suggest a link between climate change and solar variability on these time-scales, the magnitude of solar irradiance variability remains debated, as is the estimate of the role solar variability plays in Holocene climate variations (Bard and Frank, 2006).

Explosive volcanism can have a short-term cooling effect on hemispheric or global mean temperatures (Robock, 2000). If volcanic aerosols reach the stratosphere they can spread globally, reducing energy receipts at the surface, which can lead to large negative temperature anomalies in some regions, but other areas may become warmer due to circulation changes (Robock, 2000). The temperature effects are usually detectable for only 1 to 2 years after the eruption but cumulative effects from multiple eruptions closely spaced in time can last for decades (Zielinski, 2000; Schneider et al., 2009). The volcanic effect can also trigger unusually cold conditions by coinciding with other climate forcing such as reduced solar insolation (Shindell et al., 2003). Acidity records from ice cores are used as a proxy for sulfate aerosols from explosive volcanism through time (Zielinski et al., 1994). Amman and Naveau (2003) studied the frequency of tropical eruptions for the last 600 years, and with their logistic regression model they identified a 76-year cycle in compiled sulfate records from several ice cores. Reconstructions of volcanic aerosol loadings over the past 1 to 2 ka are provided by Ammann et al. (2007) and Gao et al. (2008).

1.2.2 Climate cycles in the North Atlantic region

Millennial- to decadal-scale variability during the Holcoene has been found in paleoclimate data from the North Atlantic Ocean. Bond et al. (1997) first introduced the "1500 year" cycle based on ~1500 year variablility in the concentration of lithic grains, thought to reflect the abundance of drift ice, archived in North Atlantic sediment. Bond et al. (1999) indcated that the "1500 year" cycle orginated from the same forces as the Dansgaard/Oeschger events but appeared at smaller magnitude. Since Bond et al. (1997, 2001) postulated the "1500 year cycle" as the prominent feature of the North Atlantic Holocene climate, a similar cycle has been found at several sites in North Atlantic deep sea cores (i.e. Bianchi and McCave, 1999, Chapman and Shackleton, 2000, Giraudeau et al., 2000) as well as in some terrestrial proxies from the North Atlantic region (i.e. Langdon et al., 2003, Turney et al., 2005) and in the Greenland ice-cores (Schulz and Paul, 2002, Witt

and Schumann, 2005). The orgin of the millennial scale climate cycle is still unknown and it has been debated whether the cycle is driven by solar variations, as it is correlated to variations in the production rate in cosmogenic isotopes (Bond et al., 2001), changes in oceanic circulation (Bianchi and McCave, 1999, Chapman and Shackleton, 2000, Debret et al., 2007) or to atmospheric processes linked to the North Atlantic Oscillation (Giraudeau et al., 2000). Although there is still a debate about the timing, frequency, spatial extent, and origin of the "1500 year" cycle, variability on millennial scales does exist in many Holocene paleoclimate data from the North Atlantic region.

Another known pattern of variation in the North Atlantic Ocean, showing cyclicity of 60-80 years is the Atlantic Multidecadal Oscillation (AMO) (Kerr, 2000). It has its principle expression in sea surface temperature (SST) in the North Atlantic Ocean (Schlesinger and Ramankutty, 1994) and is thought to associate with small changes in the North Atlantic branch of the Thermohaline Circulation (e.g. Delworth and Mann, 2000, Knight et al., 2005). Variation in AMO has affected variation in air temperature, precipitation and frequencies in storms and hurricane over North America and Europe (Enfield et al., 2001, Goldenberg et al., 2001) and has especially been linked to summer climate (Sutton and Hodson, 2005).

The North Atlantic Oscillation (NAO) is one of the dominant atmospheric modes of North Atlantic climate variability (Hurrell et al., 2003). The North Atlantic Oscillation (NAO) index, based on standardized atmospheric pressure difference between Stykkishólmur, Iceland and Lisbon, Portugal, reaches back to AD 1864. The relative strengths and positions of these systems vary from year to year and the variations appear either as a positive or negative NAO index. When the NAO winter index (December – March) is positive with high pressure difference between the two sites the westerlies and northeast trade winds are strong. When the index is negative more northerly winds are predominant (Hurrell, 1995).

A NAO record reconstructed from Greenland ice accumulation rate is characterized by non-stationary behavior. Most of the variability shows periods of 7-14 years in addition to a significant cycle of 80-90 year (Appenzeller et al., 1998). Wunch (1999) argued that there are no cycles distinguishable from the red noise in the NAO record and therefore the NAO does not show any significant cycles. Nevertheless, many records indicate that the NAO exhibits a periodic variability similar to those mentioned above (i.e. Cook et al., 1998, Jevrejeva and Moore, 2001, Wanner et al., 2001)

1.2.3 Indications for periodicities in Icelandic proxy data

Iceland is located in the North Atlantic Ocean, at the boundary between the relatively warm and saline Irminger Current, a branch of the North Atlantic Current originating in the tropics, and the cold and low-salinity East Greenland Current from the Arctic Ocean (Fig. 1A). The maritime climate of Iceland is characterized by large decadal variations associated with the location of storm tracks across the North Atlantic Ocean, which are in turn strongly affected by the Icelandic Low. Therefore, Iceland is in an ideal position for studying changes in both ocean currents and in the NAO.

Several studies have focused on periodicities in Holocene paleoclimate data from Iceland. There is evidence for ~715, 240, 170 and 100 year cycles in a magnetic record from a marine core from the North Shelf (MD99-2275) where the ~100 year cycle is correlated to the NAO mode at centennial time-scales (Rousse et al., 2006). From the same core, a bidecadal 20-25 year oscillation is indicated in a reconstruction of sea surface temperatures that are also argued to follow variability in the NAO in addition to multidecadal cycle centered at ~150 year, interpreted to be driven by the Meridional Overturning Circulation (MOC) induced by increased ENSO activity (Sicre et al., 2008 a and b). The magnetic series in a nearby marine core in North Iceland (MD-2269) shows significant cycles of ~200, 125 and 88 year, argued to be associated with solar variability (Andrews et al., 2003b). Spectral analysis from the principal components simplifying several different proxies from the MD-2269 core shows increased variability during Neoglaciation (Andrews et al., 2003a).

2 Materials

2.1 Regional Setting

Lake Haukadalsvatn is a glacier-eroded lake at the head of Hvammsfjörður, western Iceland (Fig. 1B). The 40-m-deep lake has a surface area of 3,28 km^2 and a catchment of 172 km^2, mostly above 500m asl. (Fig. 1C). The lake acts as sediment trap resulting in sedimentation rates that exceed 1.5 m/ka in the central basin. The surrounding bedrock is Tertiary basalt and the region lies outside the extant volcanic zones of Iceland (Jóhannesson, 1997). The valley of Haukadalur was depressed during glaciations (postglacial marine limit ~70m asl) and the earliest sediment fill in Haukadalsvatn is of

marine origin, before isostatic recovery elevated the valley above sea level about 10.6 ka ago (Geirsdóttir et al., 2009b). The soils around Haukadalsvatn are mostly andosols (eolian and tephra) but histosols can also been found near the lake (Arnalds and Grétarsson, 2001). Andosols are porous and have a tendency to bind organic matter that makes it fertile. On the other hand this type of soil often lacks cohesion that makes it vulnerable to disturbance that can cause landslides and erosion by wind and water (Arnalds, 2004). Historical accounts describe the valley of Haukadalur as being heavily forested at the time of settlement; today there is no forest in the valley but it is vegetated by grasses and sedges. The Haukadalur valley has been inhabited since the 10^{th} century.

2.2 The sediment cores from Haukadalsvatn

In 2003 two sediment cores (HAK03-1A and HAK03-1B) were recovered from a single site (65°03.064´N, 21°37.830´W) in Haukadalsvatn using the DOSECC GLAD-200 core rig (http://www.dosecc.org/). The cores were taken from a water depth of 38.33 m and captured the 30-m-thick sediment fill in the lake reaching bedrock at the bottom. The lower 12 meters of the core consists of rapidly deposited ice-proximal to ice-distal deglacial marine sediment overlain by 18 meter of lacustrine sediment. The cores are finely laminated containing numerous fine tephra layers throughout the core. The uppermost 16.5 meters of the core span the past 10.2 ka (dated by the Saksunarvatn tephra; Grönvold et al., 1995). Two surface cores (HAK03-G1 and HAK03-G2) were recovered from the drill site before deep coring using methods in Glew (1991). They capture the sediment-water interface and the uppermost 48 cm of sediment.

2.3 Chronology

The chronology for Haukadalsvatn is based on ^{210}Pb and ^{137}Cs in the uppermost part and tephrochronology in the remainder of the core (Geirsdóttir et al., 2009a). The age model is derived from a mixed-effect regression fit to 14 dated tephras (see Table 2 in Geirsdóttir et al., 2009a) and for the last 100 years to the ^{210}Pb age model, following the procedure of Heegaard et al. (2005), the statistical software R (http://cran.r-project.org), and a k-value of 9 (Fig. 2). The age model lies within $\pm 1\sigma$ of the control points.

2.4 Biogenic silica and total organic carbon variables

Total organic carbon (TOC) has been measured every 0.5 cm from the surface core (HAK03-1G) and every one cm for the last 10.2 ka y in HAK03-1B. The surface core was spliced to the top of the HAK03-1B core based on the TOC profiles (Geirsdóttir et al., 2009a). Biogenic silica (BSi) has been measured every ~one cm in the surface core (HAK03-1B) and every 2-10 cm in HAK03-1B with the highest resolution in the uppermost part of the core. For procedures see Geirsdóttir et al. (2009a). Due to the high sedimentation rate at the lake the two proxies afford time series of relatively high resolution. The BSi measurements provide a one sample on average every 5 years for the past 2 ka, and decadal resolution between 10 and 2 ka (Fig. 3A). The TOC measurements provide continuous TOC mg/g record at 1- to 3-year intervals for the last 2 ka, and decadal resolution between 10 and 2 ka (Fig. 4A).

Geirsdóttir et al. (2009a) argue that BSi in Haukadalsvatn is a proxy for aquatic primary productivity, which reflects warm April-May temperatures. This is based on a fairly strong correlation between the BSi record with 170-year long instrumental spring temperature record (April – May) from Stykkishólmur, a weather station close to Haukadalsvatn. TOC peaks during the last 2000 years are shown to represent an increased flux of terrestrial carbon to the lake from eolian-derived soil erosion following periods of cold summers accompanied by dry, windy winters (Geirsdóttir et al., 2009a). The interpretation is based on a strong correlation between measured high values of TOC and C:N and $\delta^{13}C$ peaks that reflect a greater proportion of terrestrial carbon. The role of wind is based on a positive correlation between TOC peaks and wind strength record from the Stykkishólmur weather station (Geirsdóttir et al., 2009a).

3 Data Analysis

3.1 Data processing

Time series analyses are used to identify the nature of the phenomenon represented by the sequence of observations and to predict future values of the time series variable (Ghil et al., 2002). In this paper three spectral methods are used to detect whether regular cyclicities exist in the paleoclimate proxies TOC and BSi over the Holocene record preserved in Haukadalsvatn.

The time series of TOC and BSi were processed prior to spectral analysis. The records were re-sampled with linear integration in Analyseries 2.0.4.2 (Paillard, 1996) to obtain evenly spaced time series. After the re-sampling both TOC and BSi records have one value every 20 years for the last 10.2 ka. The TOC measurements were done with a higher sampling resolution than the BSi measurements so it is possible to resample the TOC record with one value every 10 years. In order to have the same resolution for both records the 20-year sampling intervals is used for the TOC record unless this leads to a big difference in the results. At the 20-year sampling rate the highest frequency information available from the Haukadalsvatn's record is 0.025 (40 year cycle), according to the Nyquist frequency which is defined as 1/(2 x sampling interval). Many spectral methods assume the time series to be centered with the series oscillating positively and negatively around a zero line. Therefore the TOC and BSi records were standardized by subtracting the mean of the time series from every value and divided by the respective standard deviations.

3.2 Spectral Analysis

Spectral analyses are widely used to detect periodic or quasi periodic components in time series, which are indicated by peaks that can be distinguished from background noise (Weedon, 2003). The classic method for estimating spectral density is the periodogram that is formed by taking the Fourier transform of the autocovariance function of the time series. More advanced methods have been develped where the goal is to reduce spectral bias, variances and leakage of the spectral plot, to increase accuracy as well as adding new and more advanced features. In this paper Singular Spectrum Analysis (SSA) (Vautard and Ghil, 1989) and Multi Taper Method (MTM) (Thomson, 1982) in kSpectra 2.13 Toolkit (http://www.spectraworks.com) were both used to identify the significant periodicities in the TOC and BSi time series. In addition, the interactive wavelet analysis toolkit on http://paos.colorado.edu/research/wavelets/ (Torrence and Compo, 1998) was used to analyze how the spectral power varies over time.

3.2.1 Singular Spectrum Analysis

Singular Spectrum Analysis (SSA) is one of many spectral analyse methods that is suitable for decomposing short, noisy signals into a (nonlinear) trend, oscillatory components and noise (Ghil et al., 2002). The first step is to embed the time series into phase space of M

dimensions. After that, the data are treated as a series of variables, one for each embedding dimension, and a matrix is formed of the variance and covariance for every dimension being considered. The covariance matrix is diagonalized and the eigenvalues are ranked in decreasing order but the eigenvalue gives the variance of the time series in the direction specified by the corresponding eigenvector. The square root of the eigenvalues gives the singular values, which are plotted up in decreasing order to form a singular spectrum (Vautard and Ghil, 1989). The singular spectrum is used to separate signal from noise by defining components with the most variance significantly larger than other components that are identified as noise. This method works well if the noise is likely to be white noise, but in climatic and geophysical time series the noise is usually red noise which tends to have larger power at lower frequencies. Then it is necessary to use significance tests such as Monte Carlo SSA (Allen and Smith, 1996), which tests significance against a red-noise hypothesis. The eigenvalues and eigenvectors define empirical orthogonal function (EOFs) in phase space. It is possible to project the time series onto each EOF to get the corresponding principal components that can be plotted up as reconstructed components (RCs) in time space, which preserve amplitude, frequency and phase of the time series (Vautard and Ghil, 1989).

Here the SSA analysis is used for both BSi and TOC variables to filter out (non-linear) trends and oscillations with long periods relative to the length of the time series prior to the analysis. Also to test for significant periodicities in the series and to reconstruct the significant components, found in the spectrum, in the time domain. The embedding dimensions M=51, is based on number of data points and the oscillatory periods under investigation. The covariance matrix is calculated with the V&G method (Vautard and Ghil, 1989) in kSpectra. The Monte Carlo significance test is used where the error bars represent 90% of the variance.

3.2.2 Multi Taper Method

Multi Taper method (MTM) is used to reduce the variance of spectral estimates by using a small set of tapers (Thomson, 1982). The tapers are known as discrete prolate spheroidal sequences or Slepian sequences and are constructed to minimize the spectral leakage due to the finite length of the time series. The purpose of the MTM is to produce a power spectrum with small bias, good smoothing and yet high frequency resolution. A number of tapers are chosen according to the data analyzed depending on the length of the data sets

and other properties of the time series. The choice of bandwidth and number of tapers reflects the classical trade off between spectral resolution and the stability of the spectral estimate (Thomson, 1982). A set of independent estimates of the power spectrum is computed by pre-multiplying the data by each orthogonal taper and then the total power spectrum is computed by averaging the individual spectra. The peaks that appear in the power spectrum are tested for significance relative to the null hypothesis of a red-noise background estimated from the data (Mann and Lees, 1996). Confidence levels relative to the estimated red-noise background can be determined from the appropriate quantiles of the chi-squared distribution.

In the MTM analyses of the BSi and TOC time series, 5 tapers are used and the bandwidth is 3, based on the length and resolution of the records. Confidence levels of 90, 95 and 99% are used to determine significant peaks. The results from the MTM power spectrum and the SSA are used together to obtain more confident and reliable results.

3.2.3 Wavelet analysis

Wavelet analyses are used to analyze how periodicities change over time and are applicable to time series that do not contain stationary power at definite frequencies. The time series is decomposed into time-frequency space by using a wavelet, an orthogonal function where the oscillations die away to zero rather than going on indefinitely. An appropriate mother wavelet function is chosen, that can be stretched and translated with flexible resolution in both frequency and time space, and multiplied with the times series to produce a wavelet transform (Torrence and Compo, 1998).

The mother wavelet used for the BSi and TOC time series is Morlet wavelet, which is one of the most commonly used continuous wavelets in geophysics (Lau and Weng, 1995). It is a complex continuous wavelet formed by a sine wave multiplied by Gaussian envelope and the wavelet parameter used is $w_0 = 6$, which gives the number of oscillations within the wavelet itself. The wavelet scale width is 0.25 and smallest scale is 2 times the sampling interval. The data are padded with zeros at both ends to limit the edge effect; cone of influence is included to mark the region where zero padding has reduced the variance so the results are not as reliable as at the rest of the wavelet spectrum. Background spectrum is red noise and the peaks in the wavelet power spectrum above this background spectrum were assumed to be real features using a 90% significance threshold.

4 Results

4.1 Low frequency trend in the BSi and TOC records

A long-term trend, thought to obscure the higher frequency cycles, was subtracted from both the BSi and TOC series prior to the spectral analysis. The SSA was used to identify the trend/cycles of low frequency relative to the length of the series and to filter it out. In the BSi time series the first SSA component that defined a ~4000 year cycle (Fig. 3B) contained 53 % of the total variance. This was subtracted from the time series and the residuals are considered as a detrended time series (Fig. 3C). The long term trend can be described as a curve showing changes in the BSi values increasing from low values, reaching the highest BSi values in the early-mid-Holocene and declining values in the later Holocene. The trend in the BSi record, excluding the transition between the 10 and 8 ka BP from a marine to a freshwater system, broadly follows the declining summer insolation curve, with the warmest interval occurring when the summer insolation is highest and a cooling trend as summer insolation decreases (Fig. 3B).

TOC increases irregularly through the late Holocene, with the highest background values in the last millennium (Fig. 4A). This pattern is the inverse of the low-frequency BSi record. Geirsdóttir et al. (2009a) argue that the late Holocene increase in TOC reflects the influx of soil carbon delivered to the lake as summer temperatures decreased and vegetation cover was diminished. The low-frequency long-term trend was removed from the TOC time series by subtracting the first SSA component (Fig. 4B) from the original series giving a residual used as detrended series (Fig. 4C), which is stable with a constant mean. The first component accounted for 67% of the total variance and was estimated as a 5000 year cycle.

4.2 Cyclicity in the BSi record

Singular Spectrum Analysis of the detrended BSi record produced four significant periodicities of ~1200, 130, 90 and 70 years at 90% significance level (Fig. 5A). In the MTM spectrum the same periods reach above the 95% significance level (Fig. 5B). The 130-year cycle peak is strongest, exceeding the 99% significance level. The 90- and 70-year cycles just exceed the 99 % significance level, and a 1200-year cycle peak reaches above the 95 % significant level. A few additional significant peaks appear in the MTM

spectrum including 200-, 160- and 80-year peaks, but they do not exceed the 90% significant level in the SSA spectrum.

To analyze how the periodicities in the BSi record have changed over time we use wavelet analysis and reconstructions of the statistically significant components from the SSA spectrum as a function of time. A significant period of ~1200 years is present across most of the wavelet power spectrum (Fig. 6E), except a short break between 3.5 and 5 ka BP. This is similar to the reconstructed 1200-year cycle from the SSA spectrum (Fig. 6D). The 1200-year cycle component accounts for 33% of the total variance in the SSA spectrum and is rather steady through time, although with the weakest contribution around 5 ka. Most of the power at shorter periods in the wavelet is concentrated within a 100-200 year band that shows the strongest power from 4.5 to 2 ka and from 8 to 9 ka that is similar to the 130-year component in the SSA spectrum (Fig. 6C). The 130-year cycle component, with 10% of the total variance, shows the strongest power from 5.5 to 2 ka BP in the SSA reconstruction, and is also strong from 9 to 8 ka BP and for the last 0.5 to 1 ka. Although the 130-year cycle only accounts for small amount of the total variance, this peak has the greatest power in the MTM and SSA spectrum. At 2 ka, cycles of higher frequency dominate in the wavelet (Fig. 6E),which is comparable to the ~70- and 90-year cycles in the power spectra. The higher frequency components (90- and 70-year cycle) only account for 2.0% and 1.3% of the total variance in the SSA spectrum. These cycles are strongest in the later part of the record (Figs. 6A and B). The 90-year cycle shows the most power during the last 3 ka (Fig. 6B), whereas the 70-year cycle is more uniform over the whole period, although with a flat signal between 8-5 ka (Fig. 6C).

The main cyclicities in the BSi record appear in all three methods; these are 1200-, 130-, 90- and 70-year cycles. These four components account for 47% of the total variance of the original data and reconstruct the BSi record relatively well (Fig. 7). The 1200-year cycle continues through the entire record, whereas the 130-year cycle is the most significant peak in the power spectrum. In the early Holocene low-frequency cycles dominate the BSi record, whereas higher frequencies become more prominent in the late Holocene.

4.3 Cyclicity in the TOC record

In the SSA spectrum for the TOC record cycles at ~220, 47 and 40 years are significant at the 90% level (Fig. 8A), although collectively they only account for 10.5% of the total variance, much less than in the BSi SSA. The same three cycles can also be found in the MTM spectrum (Fig. 8B). A 40-year cycle reaches highest above the 99% significant level while the 220 and 47 year cycle just exceed it. In addition to these three cycles that are common to both methods, ~80 and 70 year cycles reach above the 95 % significant level and ~1200 year cycle passes above the 90% significant level in the MTM power spectrum.

Variations of the periodicities in the TOC record through time are provided by the wavelet power spectrum and in reconstructions of the significance components from the SSA spectrum as functions of time. Most power at longer periods in the wavelet power spectrum is concentrated within a ~200 to 500-year band (Fig. 9D) that is significant at the 90% level. These cycles appear between 9-8 ka and again for the last 2 ka, which is similar to how the 220-year component shows up in the SSA spectrum. The 220 year cycle accounts for 5.6% of the total variance and shows the strongest power from 9 to 7 ka and for the last ~2 ka in the SSA reconstruction (Fig. 9C). Cycles of higher frequency characterize the last ~5 ka according to the wavelet analysis. These cycles range from 50 to 100 years, and become more frequent and stronger through time with the most power for the last 1 ka (Fig. 9D). These high-frequency cycles may correspond to the 40- and 47-year cycles in the MTM and SSA spectra but they appear as longer cycles due to poor resolution in the wavelet power spectrum. The 47-year component in the SSA reconstruction has the strongest power over the last 1.8 ka but counts only for 2% of the total variance (Fig. 9B). The 40-year component in the SSA that accounts for 3% of the variance becomes stronger during the last 5 ka, peaking in the last 2 ka (Fig. 9A).

The main cycles in the TOC record are ~220-, 47- and 40-year cycles, each appearing in at least two of the spectral methods. However, the correspondence between cyclicities identified by the three spectral analyses for the TOC record is not as strong it is for the BSi record. The main components in the TOC record account for only 11% of the total variance of the original data, and they provide a rather poor reconstruction of the TOC record (Fig. 10). Overall the TOC record is a relatively unstable series with none of the cycles appearing continuously through the whole record. The cycles show variability both

in phase and amplitude through out the record, with the higher frequency cycles more prominent over the last 2 ka.

5 Discussion

5.1 Centennial and decadal variability in the BSi and TOC variables

Spectral analyses demonstrate that proxy records from Haukadalsvatn display clear periodicities on decadal to centennial time-scales. However, the BSi and TOC time series do not show the same primary cycles. In the BSi record ~1200, 130, 90 and 70 year cycles are most apparent, whereas ~220, 47 and 40 year cycles are predominant in the TOC record (Table 1). But there are also some similarities. Two of the main cycles in the BSi record, the ~1200- and 70-year cycles, also appear as weaker signals in the TOC series, and an ~80-year cycle appears as a 95% significant peak in the MTM spectrum for both proxies.

The explanation for this difference in periodicities of the two proxies is likely to be a consequence of the differences in the primary controls on the two proxies. BSi reflects diatom productivity within the lake, where higher values indicate warm spring conditions (Geirsdóttir et al., 2009a). TOC has two competing controls, within lake primary productivity, with high TOC reflecting long, warm summers, and the delivery of soil organic matter during persistent cold summer and reduced vegetation cover in the catchment (Geirsdóttir et al., 2009a). During the early Holocene thermal maximum (HTM), both TOC and BSi are relatively high and TOC exhibits only minor variations (Figs. 3A and 4A). In contrast, following periods of cold summers accompanied by dry, windy winters (Geirsdóttir et al., 2009a) BSi values are low and TOC is elevated because of an increased flux of terrestrial carbon into the lake due to enhanced soil erosion. This would explain why higher-frequency cycles dominate the TOC record when summers are cold and unstable as in the last 2 ka and between 8.5 and 8 ka (Fig. 9).

The wavelets for the TOC series indicate an unstable condition with non-continuity of the TOC cycles (Fig. 9D). This is due to the competition between within-lake primary productivity and terrestrial soil erosion as the controlling variables on TOC. Part of the instability in the TOC record can also be attributed to frequent tephra falls from Icelandic

volcanism. Tephra mantling the catchment increases landscape instability and soil erosion bringing brief increases in terrestrial carbon to the lake. However, the TOC proxy is less sensitive during warmer times when the vegetation cover is denser and more resistant to disturbance, from both climatic and volcanic perturbations. This results in greater stability of the TOC signal in the warm early Holocene and less coherence and higher frequency cycles during the colder summer of the late Holocene.

The BSi periodicities show considerably more stability than the TOC record with some of the cycles continuous through the entire record (Fig. 6E). The spectral peaks are both more detectable and stronger in the BSi power spectrum than in the TOC record and they explain a far greater proportion of the total variance than do the TOC cyclicities. The absence of higher frequency cycles in the BSi in early and mid Holocene provide evidence for milder and less variable condition during that time. However, as summer temperatures decrease in the late Holocene the system becomes more sensitive and cycles of higher frequencies appear (Fig. 7). More intense periodicities and cycles of higher frequency also characterize the last 5ka in other paleoclimate studies around Iceland (Rousse et al., 2006, Andrews et al., 2003a and b).

5.2 The mechanism of the periodicities

The periodicities appearing in the BSi and TOC time series suggest it is possible to reconstruct the likely mechanism(s) controlling the system, and to make inferences about external and internal forces that control these mechanisms. It is clear that the BSi and TOC records are not describing the same mechanism, as the dominant cyclicities in their time series have little in common. Although the dominant cycles differ between the two proxies, there are weaker correlations that suggest both proxies partly follow a common mechanism(s). The TOC record shows non-stationary tendencies, which suggests that the forcing may also be non-stationary. This supports the hypothesis that the TOC proxy is forced by two different mechanisms.

5.2.1 Ocean and atmospheric changes recorded in the BSi and TOC records

Several cycles found in the proxy records from Haukadalsvatn show similarities to cycles identified in proxy and instrumental records from the North Atlantic, mostly related to

variability in ocean- and atmospheric-dynamics. First of all, the persistent ~1200-year cycle indicated in the BSi record is of similar length (if chronological uncertainties are accounted in) as the cycles found at many sites in the North Atlantic that have been related to the "1500-year" cycle. A cycle of comparable periodicity or ~1000-1200 year cycle does also appear as a weaker signal in the TOC record. A spectral peak of 1250-year has been identified in power spectra of magnetic series from marine core recovered from Húnaflóaáll, North Iceland Shelf (Andrews et al, 2003b). They interpret the magnetic proxy as a measure of changes in the bottom current velocity. Those similar millennial scale cycles found in the proxy records from HAK and in a proxy record describing changes in bottom current velocity North of Iceland, indicate influences of oceanographic variability to long term changes in lake primary productivity within the lake. As the ~1200 year cycle in the BSi shows stable behavior through the whole period it suggests that there is a relatively stable underlying mechanism controlling the variability. The similarity in cycle length to that in the nearby marine core suggests a common origin, changes in ocean currents. The TOC proxy does not reflect the ~1200-year signal as strongly as the BSi proxy does, most likely due to secondary terrestrial origin of the TOC that would have overprinted the 1200-year signal.

The 130-year cycle, the most powerful cycle in the BSi record, shows most power from ~5.5 to 2 ka but appears to become weaker when cycles of higher frequency (70 – 90 year cycles) take over during the last 2 ka. A very similar pattern of variability is found in a sea surface temperature (SST) reconstruction from the North Shelf of Iceland (Sicre et al., 2008b). They indicate multidecadal variability in the SST reconstruction centered at ~150 years with the strongest power between 4200 and 2500 year BP turning into a higher frequency variation of 20-25 years at more recent time (Sicre et al., 2008b). These similarities support the assumption that the 130-cycle in the BSi record is most likely correlated to the Atlantic Multidecadal Oscillation (AMO), a known pattern in SST centered in the North Atlantic Ocean. However, Sicre et al. (2008b) indicate that the large multidecadal oscillation in their SST record is controlled by the Meridional Overturning Circulation (MOC), which has been linked as the driver of the AMO (Delworth and Mann, 2000). Around 2 ka, either the 130-year cycle, linked to the AMO, changes into a shorter cycle (70 to 90 years), or another more prominent forcing mechanism takes over. In Sicre et al. (2008a and b), higher frequency cycles of 20-25 years related to variations in NAO dominate the last ~2 ka. Evidence of decadal NAO variability has been recorded in several

other sites around Iceland. A ~100-year cycle in the magnetic record from the North Shelf (Rousse et al., 2006) has been previously related to variability in the NAO. There is a possibility that the explanation of the 70-90 year cycles, found in both the BSi and TOC records during the more recent time, is a result of longer-term variations in the NAO. However pressure variations like the NAO are known to be intermittent in nature with more prominent high frequency variations. A better known cyclicity in the NAO are cycles with periodicities of 2-5, 7 and 14 years, which we are unable to detect due to the coarse temporal resolution of our proxy data. Therefore the 70-90 year cycles in the BSi and TOC record are more likely AMO related, originating from changes in ocean currents where the inertia of the system is higher than for the atmosphere, resulting in slower changes.

It is to be expected that the ~40- and 47-year cycles, the most prominent cycles in the TOC record, reflect some kind of a NAO signal or an interaction of NAO and AMO. During the late Holocene, TOC is expected to follow the NAO winter index as it is interpreted to indicate periods of cold and windy conditions that could be following variations in the NAO. The higher frequency cyclicity in the TOC record is strongest in the last part of both records, especially the last 2 ka, when the TOC values are high due to colder winters and a less stable environment. The NAO forces are known to be more powerful during the winter months (Hurrell et al., 2003) so it is likely that the NAO signal is detected in the TOC record as it is interpreted as a winter proxy reflecting dry, windy winters. However the strength of the NAO is related to fluctuations in SST (Hurrell et al., 2003), so the above mentioned mechanisms are all part of the same internal system. The cyclicity in both BSi and TOC records is probably a complex result of combinations of oceanic and atmospheric forcings.

5.2.2 Evidence of solar cycles identified in the proxy record of Haukadalsvatn sediments

Some of the cycles, particularly in the BSi record, show similarities to known solar cycles. The BSi record reflects the abundance of diatoms in the lake, which in turn is dependant on solar irradiance and nutrients. Considering the mixed source of the TOC proxy and the dependence of the BSi record on sunlight, the latter is expected to be more sensitive to solar variation. The strong correlation between the solar insolation curve and the long-term trend in BSi, as well as evidence for solar forcing of sea-surface temperature derived

from the North Icelandic Shelf (Jiang et al., 2005), reinforce that interpretation. The 130-, 80- and 90-year cycles in the BSi record, as well as the ~220-year cycles in the TOC record are similar to known solar cycles. Spectral peaks identified in power spectra of magnetic time series of the marine core MD-2269 from Húnaflóaáll, North Iceland (Andrews et al., 2003b) shelf are similar to the cycles found in the HAK proxies. The magnetic parameters reflect changes in grain sizes showing variability in the ocean currents strength. Cycles in this series of ~200, 125, 88 and 78 years are thought to be of solar origin and establishing an ocean-solar link (Andrews et al., 2003b). The long-term variations on millennial time-scale in the proxy records from HAK are likely following changes in the summer insolation. The higher frequency cycles in the proxy records from HAK could also be influenced by variations in solar irradiance, although Haukadalsvatn is also sensitive to nearby sea surface conditions that may overwhelm the relatively weak signal of solar variation. It is possible that ocean circulation changes are themselves reflecting changes in solar irradiance, thereby amplifying the proxy response to solar forcing in HAK. However it is not possible to distinguish between the solar forces and ocean-atmospheric forces, and therefore impossible to conclude what is the primary forcing of the periodicities in the BSi and TOC records.

6 Conclusion

The spectral analysis of bidecadally resolved measurements of BSi and TOC from Holocene sediments in HAK indicate a clear cyclic behavior on multi-decadal and centennial time-scales. The two proxies do not show the same primary cycles; the primary cycles in the BSi record are ~1200, 130, 90 and 70 year cycles that show relatively stable and continuous behavior through the record, whereas the main cycles in the TOC record are ~220, 47 and 40 years. Furthermore, the TOC cycles are weaker and are unstable through the record. Nevertheless, some of the significant cycles in the BSi record do appear in the TOC spectral analyses, but they fail to exceed the 90% confidence level in the SSA spectrum. The presence of weak TOC cycles at the same frequencies as strong BSi cycles does suggest that the both proxies are responding at least in part to similar forcing mechanisms. The BSi proxy is primarily reflecting primary productivity within the lake, whereas the TOC reflects lake productivity as well as the flux terrestrial soil carbon.

Soil erosion appears to exhibit threshold behavior that makes the system less stable in the late Holocene, resulting in different primary cyclicities than in the BSi record.

The cycles in the BSi are strongly influenced by ocean surface currents reflecting the maritime conditions in Iceland, but cycles consistent with solar forcing do also appear. The TOC cycles are thought to follow partly the ocean surface current forcing but are in addition sensitive to changes in the NAO as Northern Hemisphere temperatures decrease in the late Holocene. The results from the spectral analysis show similarities to spectral analyses of proxies in marine cores recovered from the northern shelf of Iceland. The similarities between these records support our contention that reconstructed cyclicities in the HAK record are strongly influence by change in nearby ocean currents. It is clear that climate proxies preserved in HAK sediment respond to known climate variability in the North Atlantic tied to changes in both oceanic and atmospheric variability.

Acknowledgements

Financial support for this project was received from The Research Fund of the University of Iceland to Áslaug Geirsdóttir, The Environmental and Energy Research Fund from the Reykjavik Energy, The Icelandic Centre for Research - RANNÍS (Áslaug Geirsdóttir contract nr #0070272011) in addition to a one year M.Sc. Grant to Ólafsdóttir from the Icelandic Research Fund for Graduate Students.

References

Allen, M. R., and Smith, L. A. (1996). Monte Carlo SSA: Detecting irregular oscillations in the presence of colored noise. *Journal of Climate* **9,** 3373-3404.

Alley, R. B., Mayewski, P. A., Sowers, T., Stuvier, M., Taylor, K. C., and Clark, P. U. (1997). Holocene climatic instability: A prominent, widespread event 8200 yr ago. *Geology* **25,** 483-486.

Amman, C. M., Joos, F., Schimel, D. S., Otto-Bliesner, B. L., and Tomas, R. A. (2007). Solar influence on climate during the past millennium: Results from transient simulations with the NCAR Climate System Model. *Proceedings of the National Academy of Sciences USA* **104,** 3713-3718.

Amman, C. M., and Naveau, P. (2003). Statistical analysis of tropical explosive volcanism occurrences over the last 6 centuries. *Geophysical Research Letters* **30,** 1210.

Andrews, J. T., Harðardóttir, J., Kristjánsdóttir, G. B., Grönvold, K., and Stoner, J. S. (2003a). A high-resolution Holocene sediment record from Hunafloaall, N Iceland margin: century- to millennial-scale variability since the Vedde tephra. *The Holocene* **13,** 625-638.

Andrews, J. T., Harðardóttir, J., Stoner, J. S., Mann, M. E., Kristjánsdóttir, G. B., and Koc, N. (2003b). Decadal to millennial-scale periodicities in North Iceland shelf sediments over the last 12000 cal yr: long -term North Atlantic oceanographic variability and solar forcing. *Earth and Planetary Science Letters* **210,** 453-465.

Appenzeller, C., Stocker, T. F., and Anklin, M. (1998). North Atlantic Oscillation dynamics recorded in Greenland ice cores. *Science* **282,** 446-449.

Arnalds, O. (2004). Volcanic soils of Iceland. *Catena* **56,** 3-20.

Arnalds, O., and Grétarsson, E. (2001). Soil Map of Iceland. Agriculture Research Institute, Reykjavík.

Bard, E., and Frank, M. (2006). Climate change and solar variability: What is new under the sun? *Earth and Planetary Science Letters* **248,** 1-14.

Bianchi, G. G., and McCave, I. N. (1999). Holocene periodicity in North Atlantic climate and deep-ocean flow south of Iceland. *Nature* **397,** 515-517.

Bond, G., Kromer, B., Beer, J., Muscheler, R., Evans, M. N., Showers, W., Hoffmann, S., Lotti, R., Hajdas, I., and Bonani, G. (2001). Persistent solar influence on North Atlantic climate during the Holocene. *Science* **294,** 2130-2136.

Bond, G., Showers, W., Cheseby, M., Lotti, R., Almasi, P., deMenocal, P., Priore, P., Cullen, H., Hajdas, I., and Bonani, G. (1997). A pervasive millennial-scale cycle in North Atlantic Holocene and glacial climates. *Science* **278,** 1257-1266.

Bond, G., Showers, W., Elliot, M., Evans, M. N., Lotti, R., Hajdas, I., Bonani, G., and Johnson, S. (1999). The North Atlantic's 1-2 kyr climate rhythm: relation to Heinrich Events, Dansgaard/Oescher cycles and the Little Ice Age. *Geophysical Monograph 12* **12,** 35-58.

Bradley, R. S. (2003). Climate forcing during the Holocene. *In* "Global change in the Holocene: approaches to reconstructing fine resolution climate change." (A. W. Mackay, R. W. Batterbee, H. J. B. Birks, and F. Oldfield, Eds.). Arnold, London.

Chapman, M. R., and Shackleton, N. J. (2000). Evidence of 550-year and 1000-year cyclicity in North Atlantic circulation patterns during the Holocene. *The Holocene* **10,** 287-291.

Cook, E. R., D'Arrigo, R. D., and Briffa, K. R. (1998). A reconstruction of the North Atlantic Oscillation using tree-ring chronologies from North America and Europe. *The Holocene* **8,** 9-17.

Cooper, M. C., O'Sullivan, P. E., and Shine, A. J. (2000). Climate and solar variability recorded in Holocene laminated sediments - a preliminary assessment. *Quaternary International* **68-71,** 363-371.

Crowley, T. J. (2000). Causes of climate change over the past 1000 years. *Science* **289,** 270-277.

Debret, M., Bout-Roumazeilles, V., Grousset, F., Desmet, M., McManus, J. F., Massei, N., Sebag, D., Petit, J.-R., Copard, Y., and Trentesaux, A. (2007). The origin of the 1500-year climate cycles in Holocene North-Atlantic records. *Climate of the Past* **3,** 569-575.

Delworth, T. L., and Mann, M. E. (2000). Observed and simulated multidecadal variability in the Northern Hemisphere. *Climate Dynamics* **16,** 661-676.

Enfield, D. B., Mestas-Nunez, A.M., Trimble, P.J. (2001). The Atlantic Multidecadal Oscillation and its relationship to rainfall and river flows in the continental U.S. *Geophysical Research Letters* **28,** 2077-2080.

Frölich, C., and Lean, J. (2004). Solar radiative output and its variability: evidence and mechanisms. *Astronomy and Astrophysics review* **12,** 273-320.

Gao, C., Robock, A., and Amman, C. M. (2008). Volcanic forcing of climate over the past 1500 years: An improved ice core-based index for climate models. *Journal of Geophysical Research* **113,** D23111, doi:10.1029/2008JD010239.

Geirsdóttir, Á., Miller, G., H., Thordarson, T., and Ólafsdóttir, K., B. (2009a). A 2000 year record of climate variations reconstructed from Haukadalsvatn, West Iceland. *Journal of Paleolimnology* **41,** 95-115.

Geirsdóttir, Á., Miller, G. H., Axford, Y., and Ólafsdóttir, S. (2009b). Holocene and latest Pleistocene climate and glacier fluctuations in Iceland. *Quaternary Science Reviews* **28,** 2107-2118.

Ghil, M., Allen, M. R., Dettinger, M. D., Ide, K., Kondrashov, D., Mann, M. E., Robertson, A. W., Saunders, A., Tian, Y., Varadi, F., and Yiou, P. (2002). Advanced spectral methods for climatic time series. *Reviews of Geophysics* **40,** 1-41.

Giraudeau, J., Cremer, M., Manthe, S., Labeyrie, L., and Bond, G. (2000). Coccolith evidence for instabilities in surface circulation south of Iceland during Holocene times. *Earth and Planetary Science Letters* **179,** 257-268.

Glew, J. R. (1991). Miniature gravity corer for recovering short sediment cores. *Journal of Paleolimnology* **5,** 285-287.

Goldenberg, S. B., Landsea, C. W., Mestas-Nunez, A. M., and Gray, W. M. (2001). The recent increase in Atlantic hurricane activity: Causes and implications. *Science* **293,** 474-479.

Grönvold, K., Óskarsson, N., Johnsen, S., Clausen, H. B., Hammer, C. U., and Bard, E. (1995). Ash layers from Iceland in the Greenland GRIP ice core correlated with oceanic and land sediments. *Earth and Planetary Science Letters* **135,** 149-155.

Heegard, E., Birks, H. J. B., and Telford, R. J. (2005). Relationships between calibrated ages and depth in stratigraphical sequences: an estimation procedure by mixed-effect regression. *The Holocene* **15,** 612-618.

Hinnov, L. A. (2000). New perspectives on orbitally-forced stratigraphy. *Annu.Rev.Earth Planet.Sci* **28,** 419-475.

Hu, F. S., Kaufman, D., Yoneji, S., Nelson, D., Shemesh, A., Huang, Y., Tian, J., Bond, G., Clegg, B., and Brown, T. (2003). Cyclic variation and solar forcing of Holocene climate in Alaskan subarctic. *Science* **301,** 1890-1893.

Hurrell, J. W. (1995). Decadal trends in the North Atlantic Oscillation: Regional temperatures and precipitation. *Science* **269,** 676-679.

Hurrell, J. W., Kushnir, Y., Ottersen, G., and Visbeck, M. (2003). An overview of the North Atlantic Oscillation. *Geophysical Monograph* **134,** 1-35.

IPCC. (2007). Intergovernmental Panel on Climate Change (IPCC) Fourth Assessment Report - Climate Change 2007. Summary for Policymakers.

Jevrejeva, S., and Morre, J. C. (2001). Singular spectrum analysis of Baltic Sea ice conditions and large scale atmospheric patterns since 1708. *Geophysical Research Letters* **28,** 4503-4506.

Jiang, H., Eiríksson, J., Schulz, M., Knudsen, K.-L., and Seidenkrantz, M.-S. (2005). Evidence for solar forcing of sea-surface temperature on the North Icelandic Shelf during the late Holocene. *Geology* **33,** 73-76.

Jóhannesson, H. (1997). Yfirlit um jarðfræði hálendis Mýrasýslu og yfir til Dala. *In* "Í fjallhögum milli Mýra og Dala Árbók Ferðafélag Íslands." (G. Á. Grímsdóttir, and Á. Björnsson, Eds.), pp. 215-226. Ferðafélag Íslands, Reykjavík.

Kerr, R. A. (2000). A North Atlantic pacemaker for the centuries. *Science* **288,** 1984-1985.

Knight, J. R., Allan, R. J., Folland, C. K., Vellinga, M., and Mann, M. E. (2005). A signature of persistent natural Thermohaline Circulation cycles in observed climate. *Geophysical Research Letters* **32,** L20708, doi:10.1029/2005GL024233.

Langdon, P. G., Barber, K. E., and Hughes, P. D. M. (2003). A 7500-year peat-based palaeoclimatic reconstruction and evidence for an 1100-year cyclicity in bog surface wetness from Temple Hill Moss, Pentland Hills, southeast Scotland. *Quaternary Science Reviews* **22,** 259-274.

Lau, K.-M., and Weng, H. (1995). Climate signal detection using wavelet transform: how to make a time series sing. *Bulletin of the American Meteorological Society* **76,** 2391-2402.

Lean, J., Beer, J., and Bradley, R. (1995). Reconstruction of solar irridiance since 1610: Implications for climate change. *Geophysical Research Letters* **22,** 3195-3198.

Mann, M. E., and Lees, J. M. (1996). Robust estimation of background noise and signal detection in climatic time series. *Climatic Change* **33,** 409-445.

Paillard, D., Labeyrie, L., and Yiou, P. (1996). Macintosh program performs time series analysis. *Eos Trans. AGU* **77,** 379.

Peristyckh, A. N., and Damon, P. E. (2003). Persistence of the Gleissberg 88-year solar cycle over the last ~12000 years: Evidence from cosmogenic isotopes. *Journal of Geophysical Research* **108,** 1003.

Robock, A. (2000). Volcanic eruptions and climate. *Reviews of Geophysics* **38,** 191-219.

Rogers, M. L., Richards, M. T., and Richards, D. S. P. (2006). Long-term variability in the length of the solar cycle. *arXiv:astro-ph/0606426v3*.

Rousse, S., Kissel, C., Laj, C., Eiríksson, J., and Knudsen, K.-L. (2006). Holocene centennial to millennial-scale climate variability: Evidence from high-resolution magnetic analysis of the last 10 cal kyr off North Iceland (core MD99-2275). *Earth and Planetary Science Letters* **242,** 390-405.

Schlesinger, M. E., and Ramankutty, N. (1994). An oscillation in the global climate system of period 65-70 years. *Nature* **367,** 723-726.

Schneider, D., Amman, C. M., Otto-Bliesner, B. L., and Kaufman, D. (2009). Climate response to large, high-latitude and low-latitude volcanic eruptions in the Community Climate System Model. *Journal of Geophysical Research* **114,** D15101, doi:10.1029/2008JD011222.

Schulz, M., and Paul, A. (2002). Holocene climate variability on centennial-to-millennial time scales: 1. Climate records from the North-Atlantic realm. *In* "Climate development and history of the North Atlantic realm." (G. Wefer, W. Berger, K.-E. Behre, and E. Jansen, Eds.), pp. 41-54. Springer-Verlag Berlin Heidelberg.

Serreze, M. C., and Francis, J. A. (2006). The Arctic amplification debate. *Climatic Change* **76,** 241-264.

Shindell, D. T., Schmidt, G. A., Miller, R. L., and Mann, M. E. (2003). Volcanic and solar forcing of climate change during the preindustrial era. *Journal of Climate* **16,** 4094-4107.

Sicre, M.-A., Jacob, J., Ezat, U., Rousse, S., Kissel, C., Yiou, P., Eiríksson, J., Knudsen, K. L., Jansen, E., and Turon, J.-L. (2008a). Decadal variability of sea surface

temperatures off North Iceland over the last 2000 years. *Earth and Planetary Science Letters* **268,** 137-142.

Sicre, M.-A., Yiou, P., Eiríksson, J., Ezat, U., Guimbaut, E., Dahhaoui, I., Knudsen, K.-L., Jansen, E., and Turon, J.-L. (2008b). A 4500-year reconstruction of sea surface temperature variability at decadal time-scales off North Iceland. *Quaternary Science Reviews* **27,** 2041-2047.

Sonett, C. P., and Finney, S. A. (1990). The spectrum of radiocarbon. *Philosophical Transaction of the Royal Society of London* **30,** 413-426.

Stuvier, M., and Braziunas, T. F. (1993). Sun, ocean, climate and atmospheric 14CO2: an evaluation of causal and spectral relationships. *The Holocene* **3,** 289-305.

Sutton, R. T., and Hodson, D. L. R. (2005). Atlantic Ocean forcing of North American and European summer climate. *Science* **309,** 115-118.

Thomson, D. J. (1982). Spectrum estimation and harmonic analysis. *Proceedings of the IEEE* **70,** 1055-1096.

Torrence, C., and Compo, G. P. (1998). A practical guide to wavelet analysis. *Bulletin of the American Meteorological Society* **79,** 61-78.

Turney, C., Baillie, M., Clemens, S., Brown, D., Palmer, J., Pilcher, J., Reimer, P., and Leuschner, H. H. (2005). Testing solar forcing of pervasive Holocene climate cycles. *Journal of Quaternary Science* **20,** 511-518.

Vasiliev, S. S., and Dergachev, V. A. (2002). The ~2400-year cycle in atmospheric radiocarbon concentration: bispectrum of 14C data over the last 8000 years. *Annales Geophysicae* **20,** 115-120.

Vautard, R., and Ghil, M. (1989). Singular spectrum analysis in non-linear dynamics, with application to paleoclimatic time series. *Physica D* **35,** 395-424.

Wagner, G., Beer, J., Masarik, J., and Muscheler, R. (2001). Presence of the solar de Vries cycle (~205 years) during the last ice age. *Geophysical Research Letters* **28,** 303-306.

Wanner, H., Bronnimann, S., Casty, C., Gyalistras, D., Luterbacher, J., Schmutz, C., Stephenson, D. B., and Xoplaki, E. (2001). North Atlantic Oscillation - concepts and studies. *Surveys in Geophysics* **22,** 321-382.

Weedon, G. (1993). The recognition and stratigraphic implications of orbital forcing of climate and sedimentary cycles. *In* "Sedimentology Review." (V. P. Wright, Ed.), pp. 31-50. Blackwell, Oxford.

Weedon, G. (2003). "Time-series analysis and cyclostratigraphy - Examining stratigraphic records of environmental cycles." Cambridge University Press, Cambridge.

Witt, A., and Schumann, A. Y. (2005). Holocene climate variability on millennial scales recorded in Greenland ice cores. *Nonlinear Processes in Geophysics* **12,** 345-352.

Wunsch, C. (1999). The interpretation of short climate records, with comments on the North Atlantic and Southern Oscillation. *Bulletin of the American Meteorological Society* **80,** 245-255.

Zielinski, G. A. (2000). Use of paleo-records in determining variability within the volcanism-climate system. *Quaternary Science Reviews* **19,** 417-438.

Zielinski, G. A., Mayewski, P. A., Meeker, L. D., Whitlow, S., Twickler, M. S., Morrison, M., Meese, D. A., Gow, A. J., and Alley, R. B. (1994). Record of volcanism since 7000 B.C. from the GISP2 Greenland ice core and implications for the volcano-climate system. *Science* **264,** 948-952.

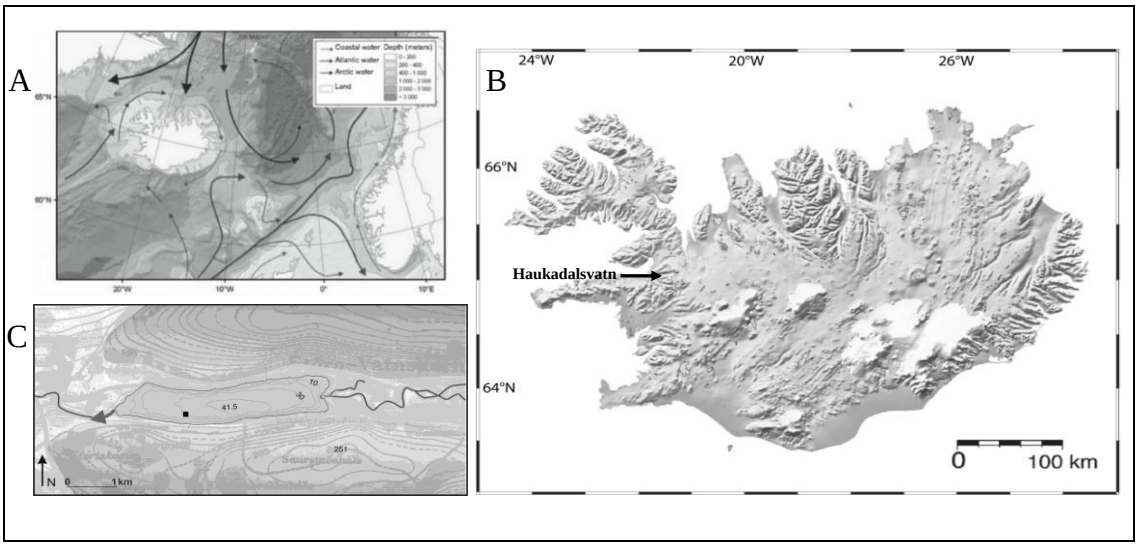

Figure 1 ***A:*** *Ocean currents in the North Atlantic region and around Iceland.* ***B:*** *Shaded relief map of Iceland showing the location of Lake Haukadalsvatn.* ***C:*** *Haukadalsvatn bathymetric map, the black square marks the coring location.*

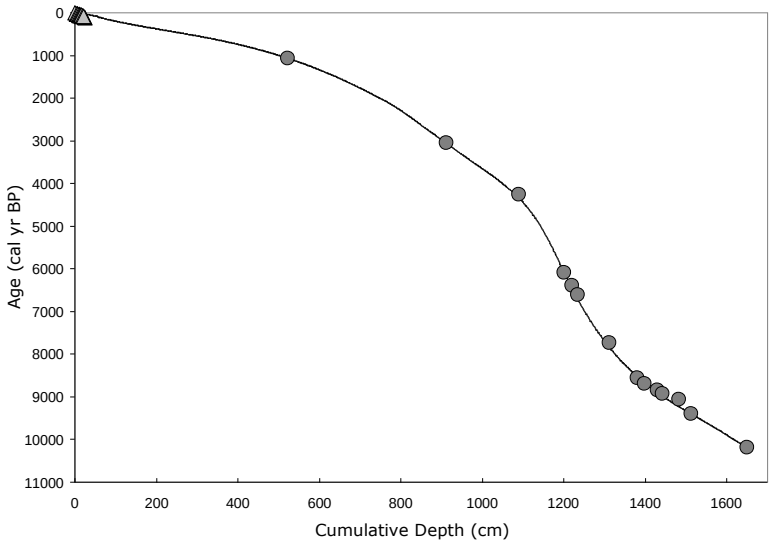

Figure 2 *The age model for core HAK03-1B from Haukadalsvatn is based on* ^{210}*Pb and* ^{137}*Cs in the uppermost part and tephrochronology in the remainder of the core. The gray circles show tephra ages and the* ^{210}*Pb age are shown with black triangles.*

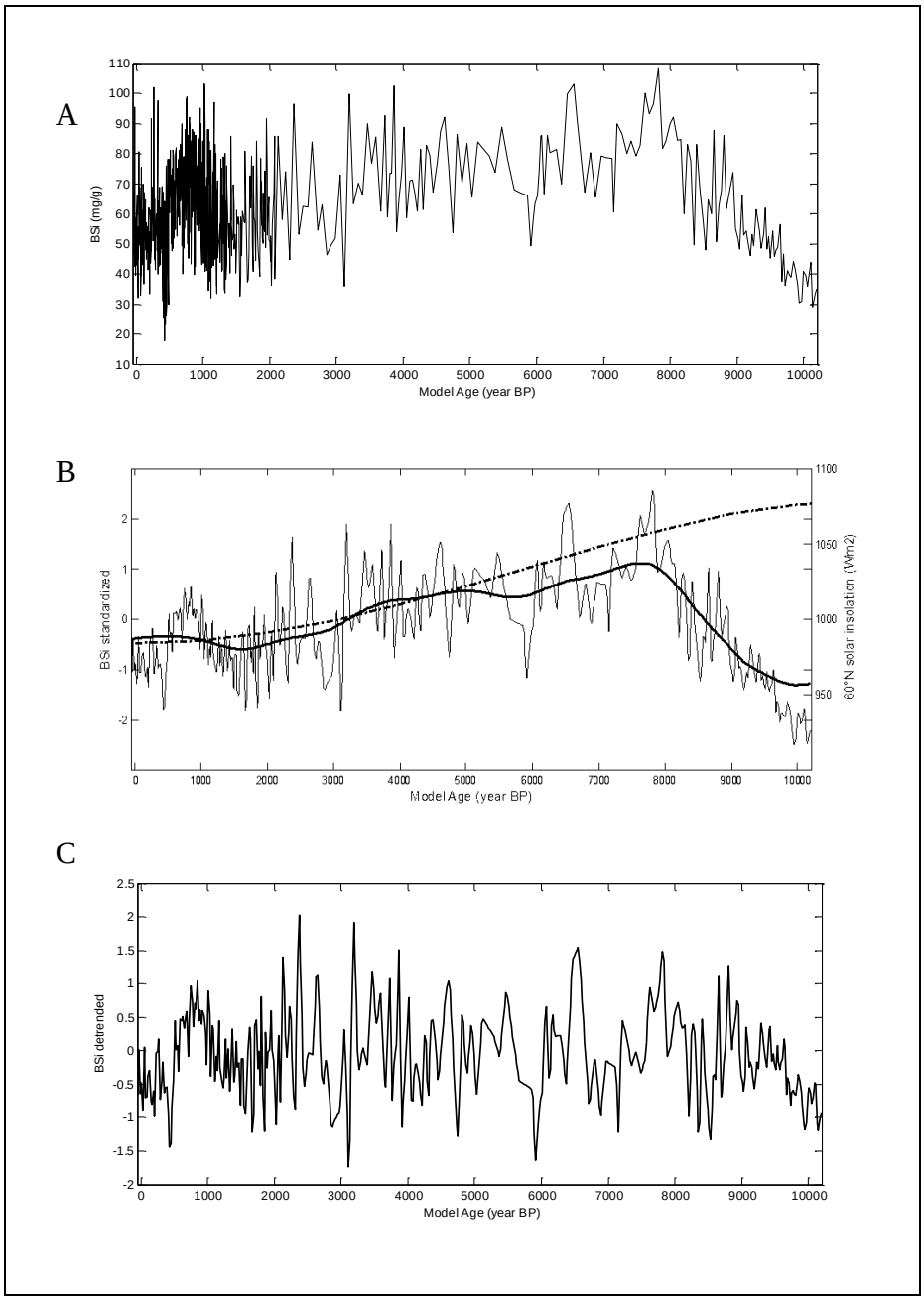

Figure 3 ***A:*** *The original raw BSi data with measurements ranging from 18-108 mg/g. The measurements provide one BSi sample on average every 5 years for the past 2 ka, and decadal resolution between 10 and 2 ka.* ***B:*** *The BSi data resampled with 20 year sampling interval (grey line) and the long time non-linear trend (black line) that was filtered out prior to the spectral analysis.* ***C:*** *The detrended BSi data that is used in the spectral analysis.*

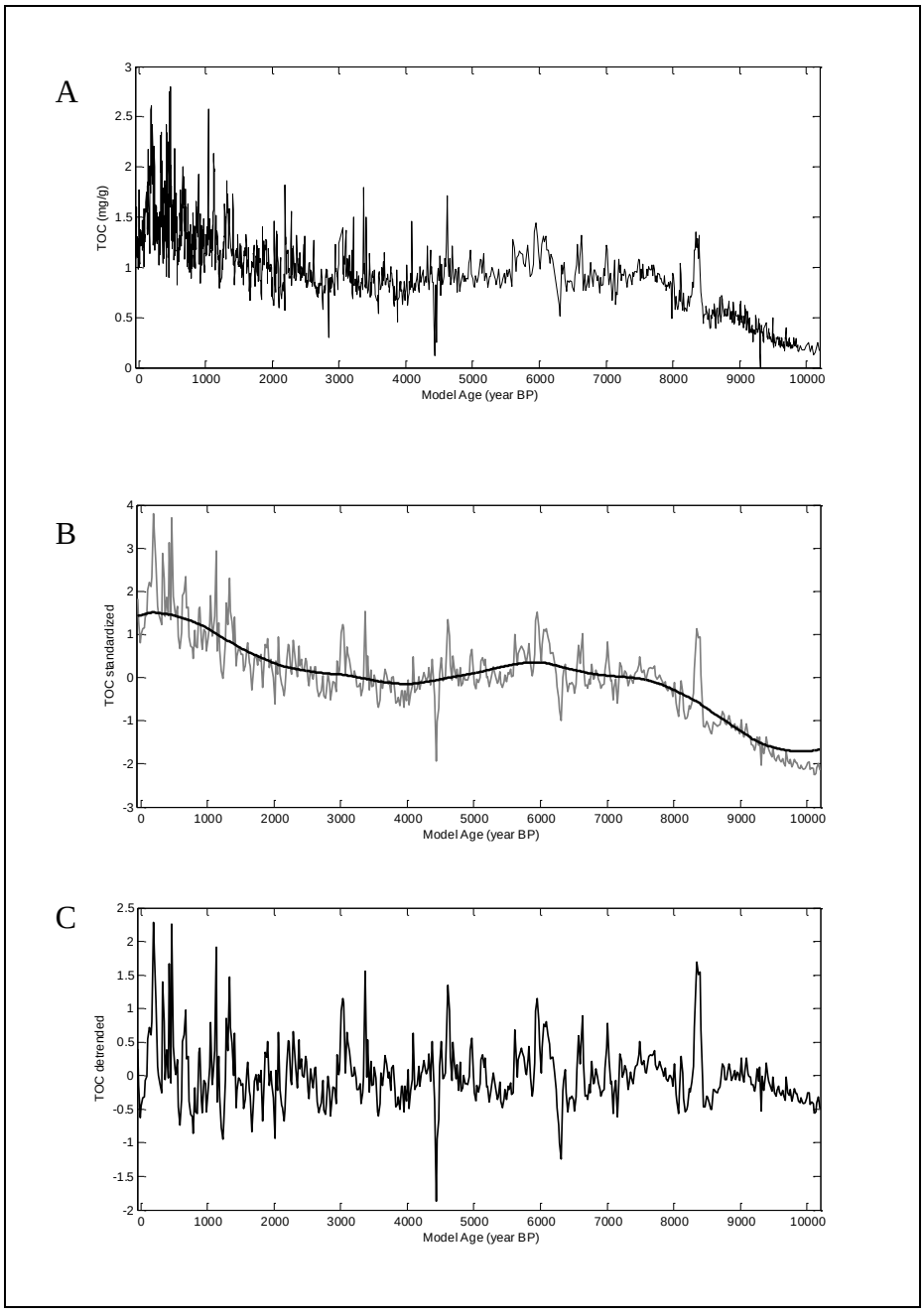

Figure 4 *TOC measurements are shown in Figure **A**, ranging from 0.3-28 mg/g. The measurements provide continuous TOC mg/g record at 1-3-year intervals for the last 2 ka, and decadal resolution between 10 and 2 ka.* ***B:*** *The TOC record resampled with 20 year time resolution (grey line) and the non-linear long term trend (black line) calculated with the SSA method, the trend was filtered out prior to the spectral analysis.* ***C:*** *The detrended TOC record that was used in the spectral analysis.*

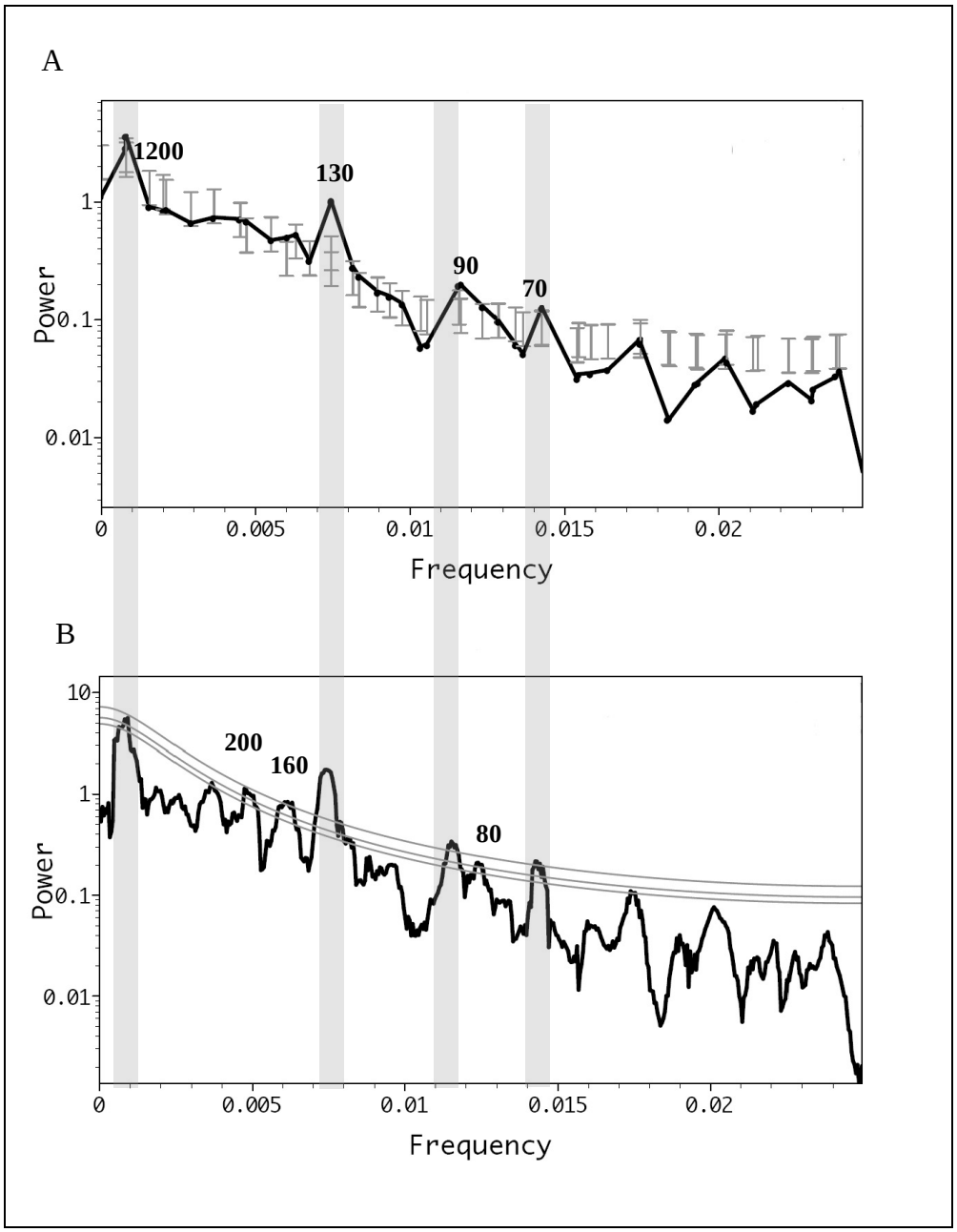

Figure 5 *Spectral Analysis for the BSi record from the sediment core from Haukadalsvatn. SSA spectrum (Figure **A**) with a 90 % significant level (grey bars) and MTM power spectrum (Figure **B**) with a 90, 95 and 99 % significant level (gray lines). Four spectral peaks are common according to both methods at ~1200, 130, 90 and 70 years (the gray areas). Additional significant peaks appear in the MTM Spectrum at 200, 160 and 80 years (Figure B).*

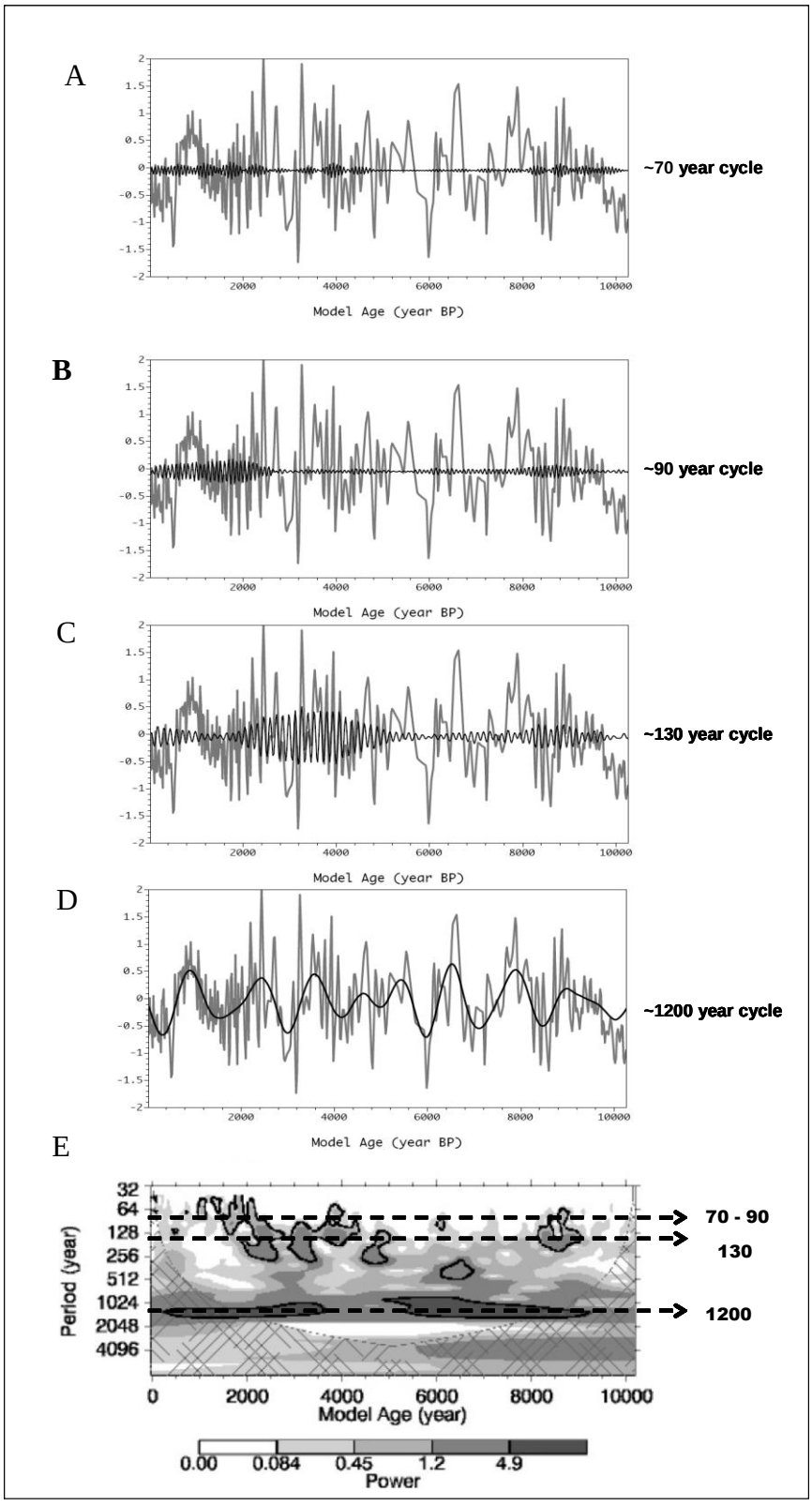

Figure 6 *The significant components from the SSA spectrum have been isolated and reconstructed as a function of time (black lines), the gray lines in the background shows the original BSi record.* ***A:*** *The ~70 year component.* ***B)*** *The ~90 year component.* ***C)*** *The ~130 year component.* ***D)*** *The ~1200 year component.* ***E:*** *Wavelet power spectrum of the BSi record for the last 10k using the Morlet wavelet. The black contour is the 10 % significant level using a red noise background spectrum and the cross-hatched region is the cone of influence. The main cycles are marked by black dashed lines.*

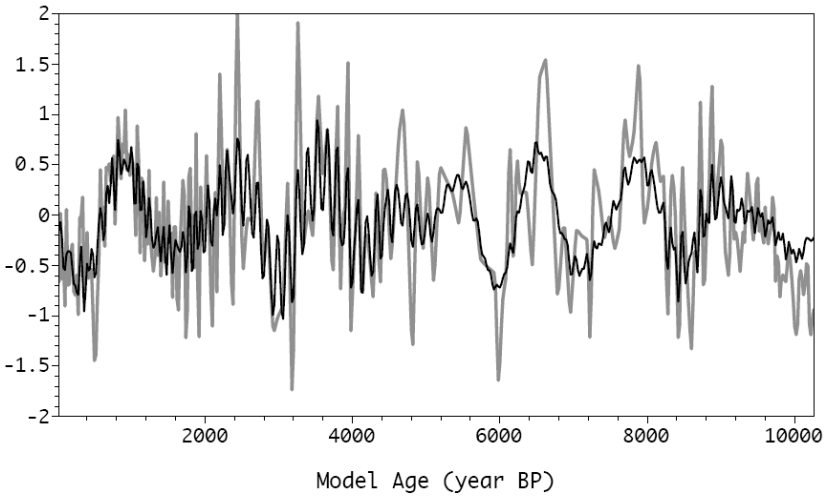

Figure 7 *The main cycles (1200, 130, 90 and 70) in the BSi record were isolated from the SSA spectrum, combined together and plotted up as a function of time (black line), the gray line shows the original BSi record. These four cycles account for 47% of the total variance of the original data and reconstruct the BSi record fairly well.*

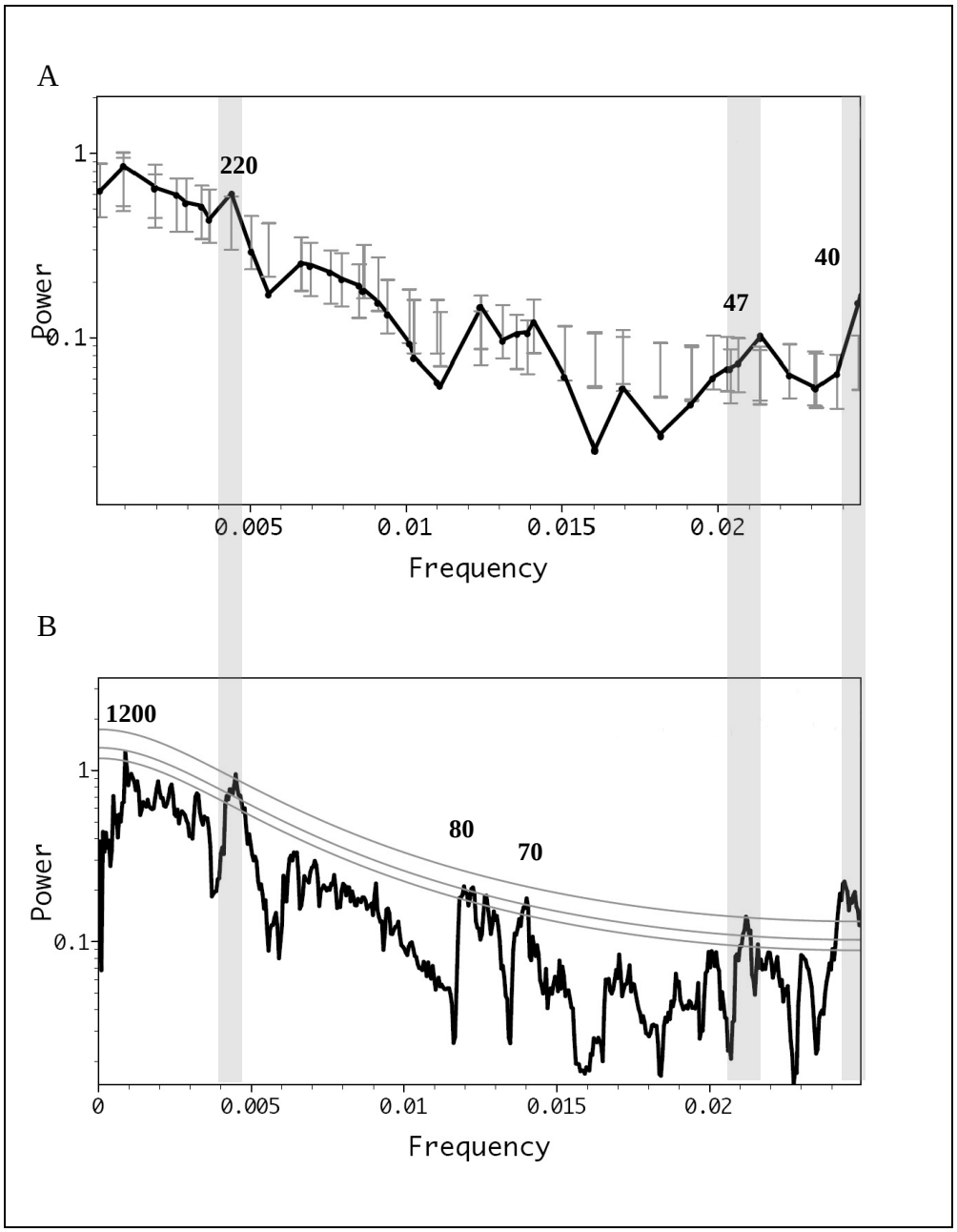

Figure 8 *Spectral Analysis for the TOC record in the core from Haukadalsvatn. Figure **A**: SSA Spectrum (black line) with a 90 % confidence level (gray bars). Figure **B**: MTM power spectrum (black line) with 90, 95 and 99% significant levels (gray lines). The common spectral peaks in both records are ~220, 47 and 40 year cycles (see the gray areas). In addition ~80 and 70 year cycles reach above the 95 % significance level and a ~1200 year cycle reaches above the 90% significant level in the MTM power spectrum (Figure B).*

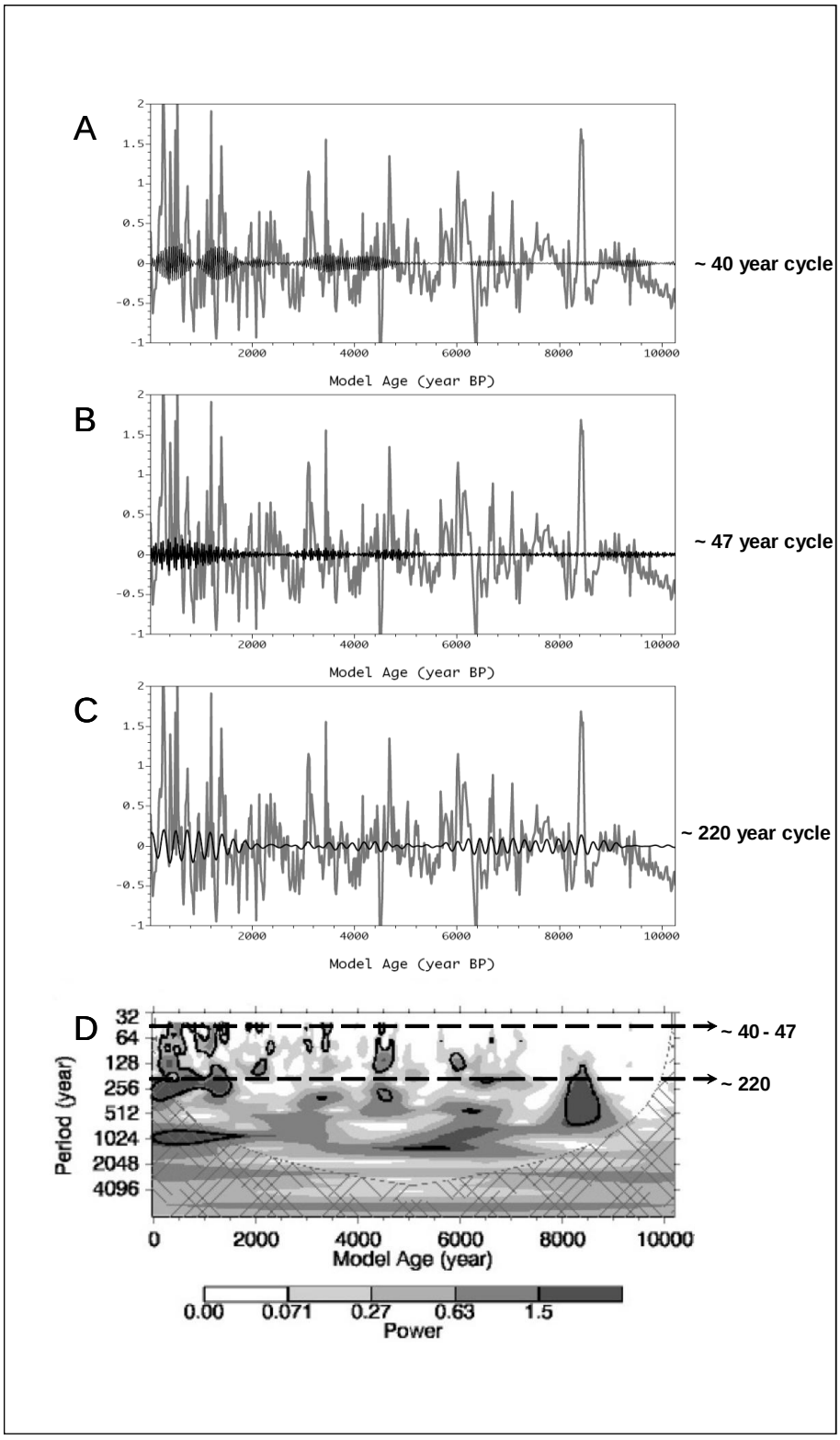

Figure 9 *The significant components from the SSA spectrum for the TOC record were isolated and reconstructed as a function of time (black lines), the gray lines in the background are the original TOC series.* ***A:*** *The ~40 year component.* ***B:*** *The ~47 year component.* ***C:*** *The ~220 year component.* ***D:*** *Wavelet power spectrum of the TOC record for the last 10k using the Morlet wavelet. The black contour is the 10 % significant level using a red noise background spectrum and the cross-hatched region is the cone of influence. The main cycles are marked by black dashed lines.*

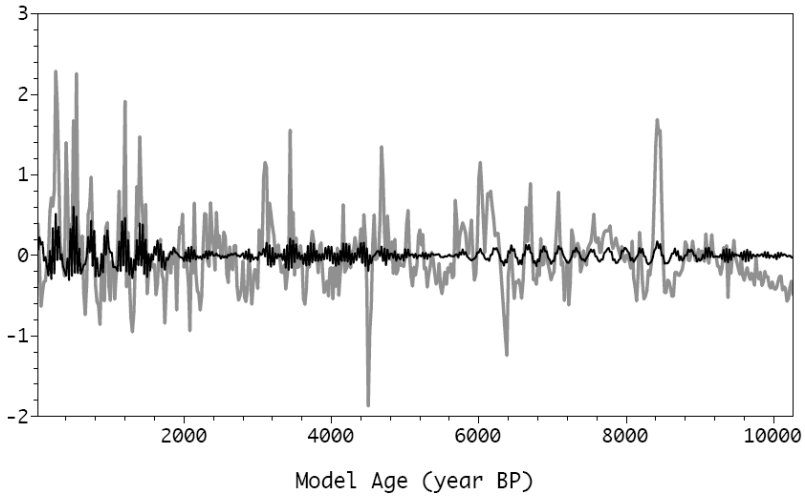

Figure 10 *The main cycles (~220, 47 and 40 year cycles) in the TOC record isolated and combined together and plotted up as a function of time (black line). The gray line is the original TOC series. These cycles in combination only account for 11% of the total variance of the TOC data which gives rather poor reconstruction of the TOC record.*

Table 1 *Significant periodicities from the BSi and TOC records indicated with the SSA method (90 % significance level) and the MTM method (99, 95 and 90% significance levels). The last row in each part of the table indicates whether the same cycles appear in the wavelet analysis. The gray areas show common cycles appearing in both the BSi and the TOC record. The bold numbers mark the main cycles in the BSi and TOC records (cycles that appear in all methods).*

	Cycles										
BSi											
SSA (90% sign)	**1200**				**130**	**90**		**70**			
MTM											
99% sign.				160	**130**	**90**		**70**			
95% sign.	**1200**		200				80				
90% sign.		270							58		
Wavelet											
appear in wavelet	**X**	X	X	X	**X**	**X**	X	**X**	X		
TOC											
SSA (90% sign)		**220**								**47**	**40**
MTM											
99% sign.		**220**								**47**	**40**
95% sign.							80	70			
90% sign.	1200										
Wavelet											
appear in wavelet		**X**					X	X		**X**	**X**

Chapter 3

Climate inferences from high-frequency cyclicity in a 3-ka varve-thickness record from Hvítárvatn, Iceland

Kristín Björg Ólafsdóttir, Áslaug Geirsdóttir, Gifford H. Miller and Darren Larsen

Abstract

A 3000-year varve-thickness record from Hvítárvatn, a glacial lake in central Iceland, preserves inter-annual variations in the delivery of glacially-eroded sediment to the lake. The first-order low-frequency trend of the varve thickness record reflects increased erosion through the Late Holocene, reaching a peak during the Little Ice Age (LIA). Superimposed on this trend are large inter-annual to decadal fluctuations in varve thickness that we suggest reflect variability in climate parameters that influence the amount of eroded sediment that is delivered to the lake each year. Here we use spectral analysis to test whether regular high-frequency cyclicity in varve thickness exists in the 3 ka varve thickness record from Hvítárvatn after removing the non-linear low-frequency variability. The spectral analyses show that dominant variations in the varve thickness record are 100 to 85, 35, 13, 5 and 2 to 4 year cycles. Some of these cycles show similar variability to that of the North Atlantic Oscillation (NAO) and Atlantic Multidecadal Oscillation (AMO). That relationship is supported by a significant correlation between varve thickness and summer NAO index as well as summer AMO index in the time domain. Comparison of the past 800 years, during which varve thicknesses are greater and more variable, with the earlier and more stable part, demonstrates that most of the dominant cycles are continuous through the entire 3ka record, both before and during the Little Ice Age. However, cycles similar to known solar cycles that appear in the early part of the

record, are not detected in the LIA portion of the time series, suggesting that higher frequency solar variability played a minor role in climate forcing during the LIA.

1 Introduction

Warming at northern latitudes has increased over the past several decades and is shown to be greater than at lower latitudes (IPCC 2007). Warming has already resulted in significant changes in the Arctic environment, including reduced sea ice cover, rapidly retreating glaciers, warmer ocean temperatures, lengthening of snow-free season and thawing permafrost. The intensification of warming in the Arctic may be explained in part by positive feedbacks associated with decreasing sea ice and thawing of permafrost, which further speeds up the melting of glaciers and ongoing rise of global sea level. Decadal-scale climate variability may also play an important role (Kerr, 2000). High-resolution proxy data that can be used to reconstruct temperature variability through time is essential in order to estimate the amplification of present warming compared to previous times. Annually laminated (varved) lake sediment records from proglacial or ice-contact lakes are ideal archives for paleoclimate reconstructions, as they offer secure chronological constraints in addition to the possibility to use changes in varve thickness as a climate proxy. A single varve consists of two primary layers: a thick layer of silt and sand, which forms in the spring and summer during the melting season, and a thin layer of clay deposited in winter when the lake is mostly ice-covered. Thicker varves are the result of increased annual production of sediment or increased efficiency in the delivery of eroded sediment to the lake. Usually, summer layers show more thickness variability than do winter layers. In many cases varve thickness is related to changes in temperature and/or precipitation during the melt season (Ohlendorf et al., 1997, Blass et al., 2007, Bird et al., 2009, Cook et al., 2009, Loso, 2009, Thomas and Briner, 2009). However, centennial-scale changes in varve thickness are also often used to describe changes in glacier size, and the position of the glacier relative to the lake (Desloges and Gilbert, 1994, Leonard, 1997, Ohlendorf et al., 1997, Hodder et al., 2007, Tomkins et al., 2008). The annual time resolution of a varved record makes it ideal to investigate climate cycles on annual to decadal time-scales. Recently, interest has been growing to recover high-resolution Holocene paleoclimate records that preserve cyclicities of high-frequency variability that can be useful for interpreting forecasts of future climate change (Weedon, 2003,

Burroughs, 2003). In addition, such high-resolution records may allow separation of natural climatic variability from a range of anthropogenic forcings.

Iceland is an ideal region for studying high-frequency variability in ocean currents, atmospheric dynamics, and the interactions between ocean and atmosphere. Iceland is located at the boundary between the relatively warm and saline Irminger Current, a branch of the North Atlantic Current originating in the tropics, and the colder and low-salinity East Greenland Current from the Arctic Ocean. The climate in Iceland is sensitive to changes in storm tracks, and is strongly affected by the Icelandic Low, a semi-permanent low pressure centre which forms one pole of the North Atlantic Oscillation (NAO). In addition, a unique geological position of Iceland on the North Atlantic ridge results in frequent volcanic eruptions creating numerous tephra layers that are preserved in the lake sediments of Iceland and serve as precisely dated horizons to constrain sedimentation age models.

Here we present spectral analyses of a 3000-year long annually laminated (varved) sediment record from Hvítárvatn, a glacier-dominated lake in central Iceland. The varve record in the Hvítárvatn system is controlled by the overall erosive power of Langjökull, second-largest ice cap in Iceland. Numerous meltwater streams draining the ice cap deliver glacially eroded sediment into Hvítárvatn. By constraining the varve counts with known tephra layers, a well-determined age model has been obtained for Hvítárvatn´s sediment archive. The varves have been counted and varve thicknesses measured for the past ~3ka (Larsen et al., in prep.). The aim of this paper is to test whether coherent inter-annual to decadal variations are superimposed on the long-term trend in the varve-thickness record, which is interpreted to be a proxy for glacier erosive power. A meteorological record covering the last ~50 years from Hveravellir, a nearby weather station ~35 km from the lake, is spliced to the much longer Stykkishólmur record (~150 km from the lake) to develop a ~200-year instrumental record to test correlations between varve thickness and specific climate variables.

The spectral analyses are used to test whether high-frequency variations in the varve record show regular periodicities, and if so, whether the cycles change over time, and to evaluate possible connections to known cycles.

2 Regional setting

Hvítárvatn (elev. 421m asl, area 28.9 km^2, max. depth 83 m) is located on the eastern margin of Langjökull, Iceland's second largest ice cap (Fig. 1). Runoff to the lake is dominated by melt water from Langjökull; in addition, two outlet glaciers, Norðurjökull and Suðurjökull, terminated in the lake during the Little Ice Age (LIA; Fig. 2). Norðurjökull has been calving into the lake since the LIA, whereas Suðurjökull retreated from the lake around 1950 AD. Fluctuations in the two outlet glaciers reflect climate change, as they are not known to be surging glaciers and there has not been active volcanism affecting this portion of Langjökull during past 3 ka. The varve thicknesses record the sediment flux to lake, which is dominated by changes in the erosive power of Langjökull, modulated by shorter-term fluctuations in the efficiency of the subglacial hydrologic system to deliver the eroded sediment to the lake.

3 Materials and methods:

Here we focus on the higher frequency variations in the varve-thickness record that are expected to reflect the modes of variability on decadal to century time-scales. The varve record use for spectral analysis was measured in a sediment core obtained from Hvítárvatn in 2003 (GLAD4-HVT03-2A; 64°38.60 N, 19°50.98 W; Fig. 2). This core was recovered from a hyaloclastite ridge, over which 15 meters of sediment has accumulated since deglaciation, with no indication of disturbances. Because the flat-topped ridge lies ~10 m above the adjacent lake floor, sedimentation is from suspension settling, avoiding complicating effects from sediment density flows that effect the main lake floor. The thickness of each annual lamina (varve) from this core more accurately represents the annual sediment flux to the lake than would varves from cores recovered from the central deep. Varves have been counted and varve thicknesses measured for the past 3000 years of sedimentation (the upper 9.65 m of the sediment core; Larsen et al., in prep.). The first-order trend of the varve thickness record is believed to reflect changes in amount of glacial erosion occurring in the lake's catchment, which is a proxy for the size of Langjökull. Tephrochronology and cross-correlation techniques on distinctive tephra and laminae patterns of four sediment cores taken from the northern basin of Hvítárvatn (Fig. 2) confirms the annual nature of the laminae in the lake (Larsen et al., in prep.). The part of

the core focused on in this study covers the time interval from 2002 AD to 830 BP with 2832 data points. The time series had 32 missing values that were estimated with a linear integration to obtain a continuous record. The sampling interval is 1 year, so according to the Nyquist frequency (1/2 * sampling interval), the shortest cycle that can be obtained from the time series has a length of 2 years, although the significance of cycles containing fewer than 4 data points per oscillation are viewed with caution, as the cycle might be a product of aliasing.

We use spectral analysis to determine whether there are regular high-frequency cyclicities in varve thickness over the past ~3 ka. Singular Spectrum Analysis (SSA; Vautard and Ghil, 1989) and Multi-Taper Method (MTM; Thomson, 1982) in kSpectra 2.13 Toolkit (spectraworks.com) were used to identify the significant periodicities in the time series. The objective was to explore the potential climate significance of the high frequency signal in the varve-thickness record. To prevent the results from becoming overwhelmed by the low-frequency terms we filtered out the low frequency components prior to spectral analyses. The SSA was used to filter out non-linear components with periods that are long relative to the length of the time series. The method was also used to calculate a Singular Spectrum to test for significant periodicities within the time series. The embedded dimension used in the SSA analysis was M = 284, based on the number of data points and the oscillations under investigation. The covariance matrix is calculated with the V&G method (Vautard and Ghil, 1989) and the Monte Carlo test was used where the error bars represent 95% of the variance.

The MTM power spectrum was calculated with 7 tapers and a bandwidth of 4 in order to obtain optimal frequency resolution without adversely affecting the stability of the spectral estimate. Confidence levels of 90, 95 and 99% relative to estimated red-noise background were used to detect significant peaks in the spectrum (Mann and Lees, 1996). The results from the MTM power spectrum were used together with the results from the SSA spectrum to obtain more reliable results.

In addition to the SSA and MTM methods the interactive wavelet analysis toolkit (http://paos.colorado.edu/research/wavelets/); Torrence and Compo, 1998) was used to analyze how the spectral power varies over the whole time period. The varve thickness data was log transformed prior to the wavelet analysis in order to stabilize the variance. The Morlet mother wavelet was used, which is the most commonly used wavelet in geophysics (Lau and Weng, 1995). The wavelet parameter used was w_0=6 and the wavelet

scale width was 0.25 with the smallest scale 2 times the sampling interval. The data were padded with zeros at both ends to limit the edge effect; a cone of influence is included to mark the region where zero padding has reduced the variance so the results are not as reliable there as for the rest of the wavelet spectrum. Background noise was red noise and the peaks in the wavelet power spectrum above this background spectrum were assumed to be real features using a 90% significance threshold.

4 Results

4.1 Long term variation in the varve thickness record

The Hvítárvatn (HVT) varve-thickness record contains a non-linear low-frequency trend that is characterized by a general increase in varve thickness that occurs in steps during the latter half of the record (Fig. 3a). Detrending is necessary to avoid the low-frequencies obscuring the higher frequency signals. Due to the non-linear behavior of the low-frequency signals, the common detrending method of subtracting a linear least squares regression line from the data is inappropriate. Instead, the SSA method was used to identify components with trend-like behavior or periodicities that are long relative to the length of the series. The first two components in the singular spectrum analysis define a ~1000 year cycle and a ~500 year cycle (Fig. 3a). The 1000-year cycle describes a slow increasing trend in varve thickness that begins in the latter half of the record, after relatively stable low-frequency behavior in the first half of the record. The 500-year cycle describes three bumps that increase in size over the past ~1500 years. Together those two components account for 57 % of the total variance of the series. The 1000- and 500-year components were combined together and then subtracted from the raw time series. The residuals (Fig. 3b) were used for the spectral analyses described below.

4.2 High-frequency cyclicity on annual to decadal time-scales

The results from the MTM power spectrum and the SSA for the varve thickness record are used together to obtain the greatest reliability in the results. These analyses indicate that the detrended varve thickness record contains regular cyclic behavior at several frequencies. The SSA power spectrum of the detrended varve-thickness record shows several significant components at a 95 % significance level (Fig. 4a). A decadal cycle of

83 to 110 years is indicated in the spectrum, in addition to a relatively strong cycle of 34 years. Components at 12.8, 5 and 4.4 years appear significant, as well as several higher frequency cycles between 2 and 4 years. However, the strongest and most prominent component in the Singular Spectrum for the varve-thickness record is a 2.8-year cycle that reaches high above the significance threshold (Fig. 4a).

Similar cycles are detected in the MTM power spectrum for the detrended varve thickness as in the SSA spectrum. Spectral peaks at 110, 34, 12.8, 5 and 4.4 years that rise above a 99% confidence threshold (Fig. 4b) are also significant cycles in the SSA spectrum. Two additional significant cycles at 55 and 9.7 years are found in the MTM spectrum, cycles that do not pass above the 95% significance test in the SSA spectrum. A number of high-frequency spectral peaks showing cyclicities between 2 and 4 years reach above 95 and 99% significance thresholds in the MTM spectrum, with a 2.8-year cycle the most powerful spectral peak in the whole spectrum, extending well above a 99% significance threshold.

Wavelet analyses were used to evaluate how the frequency power varies through time. The detrended varve thickness data was log-transformed prior to the wavelet analyses in order to stabilize the variance (Fig. 5a). Before the log transformation the amplitude of the oscillation was much larger after 1250 AD (Fig. 3b), where the varve thickness was largest prior to the detrending. The log transformation made no difference in the previous spectral analyses, but without stabilizing the variance prior to the wavelet analysis, the power was concentrated in the most recent period (after1250 AD), providing a biased evaluation of the full 3 ka record.

None of the cycles in the varve thickness series are entirely continuous in the wavelet, although a high-frequency variance between 2 and 4 years does cover most of the wavelet power spectrum except between 0 and 500 AD (Fig. 5b). Those cycles are at the same length as the high frequency cycles appearing in the MTM and SSA spectrum. Cycles of 10 to16 years appear in the wavelet spectrum mostly during the last 500 years and from 400 to 800 AD. A 30- to 40-year cycle is identified with non-stationary tendencies that evolve into longer cycles of 50 to 60 years over the last ~1400 years in the wavelet spectrum. A cycle with power concentrated within the ~100-year band is most strongly expressed around 1000 to 500 AD, but is continuous through most of the record although with lower significance.

The main periodicities in the detrended varve-thickness record, appearing in all three methods, are cycles of 100 to 85, 35, 13 to 11, 5, and 2.8 years. Although a cycle of 2.8 years is only just above the minimum cycle length that can be detected as defined by the Nyquist frequency, it appears as the strongest cycle in both the MTM and SSA power spectrum, and it is the most persistent cycle in the wavelet spectrum as well. Consequently, we consider the 2.8-year cycle very likely to be a major cycle in the varve thickness series. Overall the cycles are more prominent and stronger during the last 1500 years according to the wavelet spectrum, and the high-frequency cycles show stronger power in the most recent part.

5 Discussion

5.1 Long-term changes in glacier extent

The low-frequency trend that was filtered out prior to the spectral analysis is evaluated by Larsen et al. (in prep.). Langjökull reached its maximum Holocene position during the LIA based on a multiproxy study of the Hvítárvatn sediment (Black, 2008). Over the last century, Langjökull's outlet glaciers have been receding. Suðurjökull retreated from the lake around 1950 AD and Norðurjökull is about to leave the lake. However, the varve thicknesses have not reached the same low level as before LIA, although the sedimentation rate has decreased significantly since the ice cap started to retreat. This modest time lag has been discussed by Desloges and Gilbert (1994) and Leonard (1997), who note that glacier retreat after a maximum advance, may be characterized by succession of thick varves. This suggests that Hvítárvatn sedimentation is still recovering from the LIA expansion of Langjökull.

5.2 Understanding controls on high-frequency variations in varve thickness: a summer climate proxy

The nearest weather station to Hvítárvatn is located in Hveravellir, ~35 km north of, and ~220 m higher than the lake (Fig. 1). The instrumental record from Hveravellir goes back to 1966 AD. The temperature is usually below 0 °C at Hveravellir from October to May, and the lake is mainly ice-covered during that time. The mean annual temperature for the time period 1966 - 2002 AD is 0.9 °C, and mean cumulative precipitation is 726 mm w.e.

per year. The weather station at Stykkishólmur, located ~150 km west of, and ~400 m lower altitude than Hvítárvatn (Fig. 1), has a temperature record that extends back to 1830 AD, with a mean annual temperature of 3.4 °C. The precipitation record extends back to 1857 AD with a mean total precipitation of 692 mm w.e. per year. Although the mean temperature and precipitation is not the same as at Hveravellir for the overlap period, the variations show similar patterns. The correlation is strongest for the temperature records ($r= 0.95$; $p< 0.001$; Fig. 6a), but is somewhat weaker for the precipitation records ($r= 0.66$; $p< 0.001$; Fig. 6b). Due to the acceptable correlation between the overlapping instrumental series from Stykkishólmur and Hveravellir, we can reconstruct the Hveravellir temperatures and precipitation farther back in time. The Hveravellir records were spliced together with the Stykkishólmur records by shifting the Stykkishólmur record such that the mean values of the records from both stations match during their period of mutual overlap (1966 to 2002). The reconstructed records are a composite of the Hveravellir records for the most recent time (1966 to 2002) and the shifted Stykkishólmur records for the older part (prior to 1966). The reconstructed Hveravellir temperature and precipitation records were used to test whether there is a significant correlation between the HVT varve-thickness record and specific climate parameters (Table 1).

The best correlation between the HVT varve thickness and reconstructed Hveravellir temperature is for the summer months (June, July, August and September; Fig. 7a; Table 1). Both records were smoothed with a 3-year moving average filter prior to the correlation analysis to circumvent possible errors in the varve counts and high-frequency variations that can be local in nature in the Stykkishólmur record. The correlation is better if the temperature record is moved one year forward. Such an adjustment is thought to be within the uncertainties of the varve counts whereas there is uncertainties of both the counting‘s of the varves and in the dating of each tephra layers. Alternatively, there may be one-year lag between a warm summer and the production of a thick varve. A similar one-year adjustment improves the precipitation correlation. The strongest correlation between HVT varve thickness and precipitation is also obtained using the summer months (Fig. 7b; Table 1), especially the late summer months (July, August and September). However the correlation between varve thickness and precipitation is weaker than between varve thickness and temperature. This may be due to larger uncertainties in the measurement of precipitation. Precipitation is more locally variable than temperature, depending on the topography and distance from the sea. Consequently, the correlation

between precipitation receipts from place to place is weaker, as is seen in the relationship between the precipitation records from Hveravellir and Stykkishólmur. In addition, precipitation measurements are less certain than temperature and pressure measurements back in time, as the surroundings at the sites of measurements have changed, as has the exact location of the measurement sites (Jónsson, 2003). However, despite all the uncertainties, an acceptably significant correlation exists between varve thickness and precipitation.

Based on the strong correlations between varve thickness and summer climate (Fig. 7) we assume that the high-frequency variations in varve thickness reflect systematic changes in conditions during the melt season. During relatively warm and/or wet summers, varves are relatively thick. We hypothesize that with the additional production of meltwater, the efficiency of Langjökull's subglacial hydrologic system is increased, allowing more efficient transport of stored erosion products to the lake.

Due to the instability in the mean varve thickness record caused by changes in overall size of Langjökull, it is not possible to use the relationship between varve thickness and summer temperature to reconstruct temperature back in time. It is too complex to exactly apportion the thickness of each varve that is due to the melting influenced by air temperature and summer rainfall from the proportion of the varve that is due to the position and size of Langjökull.

5.3 Correlation with the North Atlantic Oscillation

Climate in Iceland is under the dominant influence of the Icelandic Low, a low atmospheric pressure found between Iceland and southern Greenland, which forms one pole of the North Atlantic Oscillation (NAO; Hurrell, 2003). Icelandic temperature and precipitation records show moderate but significant correlation with the NAO (Hanne et al., 2004). Based on the relationship between the HVT varve thickness and summer temperature and precipitation it is possible that the highest-frequency cycles obtained from the spectral analysis reflect summer climate variability related to the NAO. Some of the cycles indicated in the power spectrum show similar variability to that of the NAO. Known periodicities in the 130-year NAO winter index are a 3 to 5 year cycle and a 6 to 10 year cycle (Hurrel and van Loon, 1997). Wunch (1999) found weak features of 2.5 and 8 years period, but he also argued that there are no cycles distinguishable from the red noise

in the NAO record. Wanner et al. (2001) did a spectral analysis of the known NAO reconstruction from Luterbacher et al. index (2001) and revealed 2- to 10-year cycles, in addition to a longer frequency cycle of 64 years, which is also known in other NAO reconstructions (i.e. Appenzeller et al., 1998, Cook et al., 1998)

Another known pattern of variation in the North Atlantic Ocean, showing cyclicity of 60 to 80 years is the Atlantic Multidecadal Oscillation (AMO; Kerr, 2000). It has its principle expression in sea surface temperature (SST) in the North Atlantic Ocean (Schlesinger and Ramankutty, 1994). Variation in the AMO has affected air temperature, precipitation, storm frequencies, and hurricanes over North America and Europe (Enfield et al., 2001, Goldenberg et al., 2001), and has especially been linked to summer climate (Sutton and Hodson, 2005). Therefore it is likely that the longer term cycles in the HVT varve thickness series like the 55- and 85- to 100-year cycles could be related to variations of the AMO.

Correlation analysis is used to evaluate a possible link between cycles in varve thickness in Hvítárvatn and the cycles of AMO and NAO forcing. The varve thickness record is compared with the monthly station-based NAO index (Hurrell, 1995) and a AMO-index calculated from the Kaplan SST dataset (Einfield et al., 2001), where all records were smoothed with 3 year running mean to eliminate the highest frequency variations (Table 2). Due to the strong correlation between summer climate parameters and varve thickness, the mean summer values over June, July, August and September from both the AMO index (Fig. 8b) and the NAO index (Fig. 8c) were used for the comparison. Because of the observed 1-year lag between varve thickness and summer climate parameters the NAO and AMO indices were also moved one year forward to have the same identity. There is a significant correlation between varve thickness and summer AMO ($r = 0.34$; $p < 0.001$), as well as between varve thickness and summer NAO ($r = 0.28$; $p = 0.001$), which indicates that the atmospheric and ocean forces do at least partly influence the observed variations in the varve thickness. Relationships between our compiled instrumental summer temperature record (Fig. 8d) and NAO and AMO indices were also evaluate, as well as the correlation between our compiled summer instrumental precipitation record (Fig. 8e) and the NAO and AMO indices (Table 2). The summer temperatures are linked to variations in the AMO but are not significantly correlated with the NAO. On the other hand, summer precipitation does correlate with the NAO, whereas it is not significantly correlated to the AMO. As the high-frequency variations in the

varves from Hvítárvatn are influenced by both precipitation and temperature during the melting season, the underlying forces that control these terms are most likely some combination of AMO and NAO. This suggests that the cycles obtained in the varve thickness time series do reflect both NAO and AMO modes of variability expressed through the climate parameters.

5.4 Evolution of cyclicities over the past 3 ka

The mean varve thickness in Hvítárvatn increased at ~1250 AD, at the onset of the LIA (Larsen et al., in prep.). This increase in varve thickness suggests that subsequently the primary climate drivers controlling the mass balance of Langjökull were such that the ice cap was larger and more erosive for the next ~800 years. Because this may represent a fundamental reorganization of ocean-atmosphere circulation in the northern North Atlantic area, the varve thickness series was split into two segments to test whether dominant cyclicities in the spectral analyses also changed at this time (Figure 9a and d). Spectral analyses were carried out for the subperiods before and after 1250, respectively, in the same way as for the entire record. The power spectrum was calculated with MTM to identify the spectral peaks (Fig 9c and f), whereas wavelet analysis was used to analyze how, and if, the cycles changed through time (Fig. 9b and e).

The two time series show both similarities and differences. For convenience, we refer to the younger time series (after 1250 AD) as the "Little Ice Age", even though this includes the 20th Century, and the earlier time series the "early Neoglacial", even though Neoglaciation at Langjökull began substantially earlier. Our spectral comparison suggests:

1) A 100-year cycle present in the early Neoglacial is absent in the Little Ice Age, where the longest cycle is ~60 years.

2) A ~35 year cycle exists in both time series. However, cycles of 40 to 50 years are more prominent in the wavelet spectrum of the LIA, suggesting that the 35-year cycles in the early Neoglacial are transformed into a less regular and lower-frequency cycle during the LIA.

3) Cycles similar to the known 11- and 22-year solar cycles, appear in the early Neoglacial but are not present in the LIA. This suggests that non-solar forcings may be the dominant explanation for high-frequency variability during the LIA, whereas solar forcing was an important variable in the early Neoglacial.

4) The variance at 2 to 5 years that appears in the spectrum for the entire record also exists in both the LIA and early Neoglacial time series when analyzed separately. However, the strong 2.8-year cycle is only detected in the LIA portion of the record.

6 Conclusion

The varved sediment record from Hvítárvatn reflects changes in the production of glacial erosion by Langjökull and its delivery to the lake; in general, more glacial erosion results in thicker varves. Spectral analyses of detrended varve thickness series, where the influence of glacier power has been filtered out, reveal definite cyclicities. The main periodicities in the 3000-year long detrended varve thickness record, appearing in all of the three methods, are 100-85, 35, 13-11, 5 and 2.8 year cycle.

1. None of the cycles in the varve thickness series are entirely continuous in the wavelet analysis, although a high-frequency variance between 2 and 4 years does cover most of the wavelet power spectrum, with a short break between 0 and 500 AD
2. The higher frequency variations in the varve thickness record reflect climate conditions during the melt season, with a significant correlation between varve thickness and both temperature and precipitation.
3. NAO-like cycles such as 2- to 5-, and ~13-year cycles, and AMO-like cycles, such as 60 to 100 year cycles are identified in the record. This is supported by a significant correlation with summer NAO and summer AMO indices in the time domain.
4. A fundamental change in varve thicknesses occurs around the onset of the LIA, ~1250 AD. Cycles similar to known solar cycles, like the 11- and 22-year cycles, are identified before this change but are not present subsequently.
5. The results from the spectral analyses of the 3000 year long varve thickness record from Hvítárvatn suggests that different forcing controlled the record before the LIA than during the LIA. The solar forcing played a bigger role as one of the controlling factor before the LIA, but atmosphere and ocean forcing (AMO and NAO) took over during the LIA.

Acknowledgements

Financial support for this project was received from The Research Fund of the University of Iceland to Áslaug Geirsdóttir, The Environmental and Energy Research Fund from the Reykjavik Energy, The Icelandic Centre for Research - RANNÍS (Áslaug Geirsdóttir contract nr #0070272011) in addition to a one year M.Sc. Grant to Ólafsdóttir from the Icelandic Research Fund for Graduate Students. We thank Trausti Jónsson at the Icelandic Meteorological Office, for donating the extended temperature- and precipitation- records from Stykkishólmur.

References

Appenzeller, C., Stocker, T. F., and Anklin, M. (1998). North Atlantic Oscillation dynamics recorded in Greenland ice cores. *Science* **282,** 446-449.

Bird, B. W., Abbott, M. B., Finney, B. P., and Kutchko, B. (2009). A 2000 year varve-based climate record from the central Brooks Range, Alaska. *Journal of Paleolimnology* **41,** 25-41.

Black, J. L. (2008). "Holocene climate change in south central Iceland: a multiproxy lacustrine record from glacial lake Hvítárvatn." Unpublished Ph.D. thesis, University of Colorado, Boulder.

Blass, A., Grosjean, M., Troxler, A., and Sturm, M. (2007). How stable are twentieth-century calibration models? A high-resolution summer temperature reconstruction for the eastern Swiss Alps back to AD 1580 derived from proglacial varved sediments. *The Holocene* **17,** 51-63.

Burroughs, W. J. (2003). "Weather Cycles. Real or imaginary?" Cambridge University Press, Cambridge.

Cook, E. R., D'Arrigo, R. D., and Briffa, K. R. (1998). A reconstruction of the North Atlantic Oscillation using tree-ring chronologies from North America and Europe. *The Holocene* **8,** 9-17.

Cook, T. L., Bradley, R. S., Stoner, J. S., and Francus, P. (2009). Five thousand years of sediment transfer in a high arctic watershed recorded in annually laminated sediments from Lower Murray Lake, Ellesmere Island, Nunavut, Canada. *Journal of Paleolimnology* **41,** 77-94.

Desloges, J. R., and Gilbert, R. (1994). The record of extreme hydrological and geomorphological events inferred from glaciolacustrine sediments. *In* "Variability in Steam Erosion and Sediment Transport." (L. J. Olive, R. J. Loughran, and J. A. Kesby, Eds.), pp. 133-142. IAHS Publication.

Enfield, D. B., Mestas-Nunez, A.M., Trimble, P.J. (2001). The Atlantic Multidecadal Oscillation and its relationship to rainfall and river flows in the continental U.S. *Geophysical Research Letters* **28,** 2077-2080.

Goldenberg, S. B., Landsea, C. W., Mestas-Nunez, A. M., and Gray, W. M. (2001). The recent increase in Atlantic hurricane activity: Causes and implications. *Science* **293,** 474-479.

Hanna, E., Jónsson, T., and Box, J. E. (2004). An analysis of Icelandic climate since the nineteenth century. *International Journal of Climatology* **24,** 1193-1210.

Hodder, K. R., Gilbert, R., and Desloges, J. R. (2007). Glaciolacustrine varved sediments as an alpine hydroclimatic proxy. *Journal of Paleolimnology* **38,** 365-394.

Hurrell, J. W. (1995). NAO Index Data provided by the Climate Analysis Section, Boulder, USA.

Hurrell, J. W., Kushnir, Y., Ottersen, G., and Visbeck, M. (2003). An overview of the North Atlantic Oscillation. *Geophysical Monograph* **134,** 1-35.

Hurrell, J. W., and Loon, H. V. (1997). Decadal variations in climate associated with the North Atlantic Oscillation. *Climatic Change* **36,** 301-326.

IPCC. (2007). Intergovernmental Panel on Climate Change (IPCC) Fourth Assessment Report - Climate Change 2007. Summary for Policymakers.

Jónsson, T. (2003). Langtímasveiflur II. Úrkoma og úrkomutíðni (Long term variations II. Precipitation and precipitation frequency). *In* "Meteorological Office Internal Report 03010." Veðurstofa Íslands.

Kerr, R. A. (2000). A North Atlantic climate pacemaker for the centuries. *Science* **288,** 1984-1985.

Kerr, R. A. (2000). A North Atlantic pacemaker for the centuries. *Science* **288,** 1984-1985.

Lau, K.-M., and Weng, H. (1995). Climate signal detection using wavelet transform: how to make a time series sing. *Bulletin of the American Meteorological Society* **76,** 2391-2402.

Leonard, E. M. (1997). The relationship between glacial activity and sediment production: evidence from a 4450-year varve record of Neoglacial sedimentation in Hector Lake, Alberta, Canada. *Journal of Paleolimnology* **17,** 319-330.

Loso, M. G. (2009). Summer temperatures during the Medieval Warm Period and Little Ice Age inferred from varved proglacial lake sediments in southern Alaska. *Journal of Paleolimnology* **41,** 117-128.

Luterbacher, J., Xoplaki, E., Dietrich, D., Jones, P. D., Davies, T. D., Portis, D., Gonzales-Rouco, J. F., von Storch, H., Gyalistras, D., Casty, C., and Wanner, H. (2001). Extending North Atlantic oscillation reconstructions back to 1500. *Atmospheric Science Letters* **2,** 114-124.

Mann, M. E., and Lees, J. M. (1996). Robust estimation of background noise and signal detection in climatic time series. *Climatic Change* **33,** 409-445.

Ohlendorf, C., Niessen, F., and Weissert, H. (1997). Glacial varve thickness and 127 years of instrumental climate data: a comparison. *Climate Change* **36,** 391-411.

Schlesinger, M. E., and Ramankutty, N. (1994). An oscillation in the global climate system of period 65-70 years. *Nature* **367,** 723-726.

Sutton, R. T., and Hodson, D. L. R. (2005). Atlantic Ocean forcing of North American and European summer climate. *Science* **309,** 115-118.

Thomas, E. K., and Briner, J. P. (2009). Climate of the past millennium inferred from varved proglacial lake sediments on northeast Baffin Island, Arctic Canada. *Journal of Paleolimnology* **41,** 209-224.

Thomson, D. J. (1982). Spectrum estimation and harmonic analysis. *Proceedings of the IEEE* **70,** 1055-1096.

Tomkins, J. D., Lamoureux, S. F., and Sauchyn, D. J. (2008). Reconstruction of climate and glacial history based on a comparison of varve and tree-ring records from Mirror Lake, Northwest Territories, Canada. *Quaternary Science Reviews* **27,** 1426-1441.

Torrence, C., and Compo, G. P. (1998). A practical guide to wavelet analysis. *Bulletin of the American Meteorological Society* **79,** 61-78.

Vautard, R., and Ghil, M. (1989). Singular spectrum analysis in non-linear dynamics, with application to paleoclimatic time series. *Physica D* **35,** 395-424.

Wanner, H., Bronnimann, S., Casty, C., Gyalistras, D., Luterbacher, J., Schmutz, C., Stephenson, D. B., and Xoplaki, E. (2001). North Atlantic Oscillation - concepts and studies. *Surveys in Geophysics* **22,** 321-382.

Weedon, G. (2003). "Time-series analysis and cyclostratigraphy. Examining stratigraphic records of environmental cycles." Cambridge University Press, Cambridge.

Wunsch, C. (1999). The interpretation of short climate records, with comments on the North Atlantic and Southern Oscillation. *Bulletin of the American Meteorological Society* **80,** 245-255.

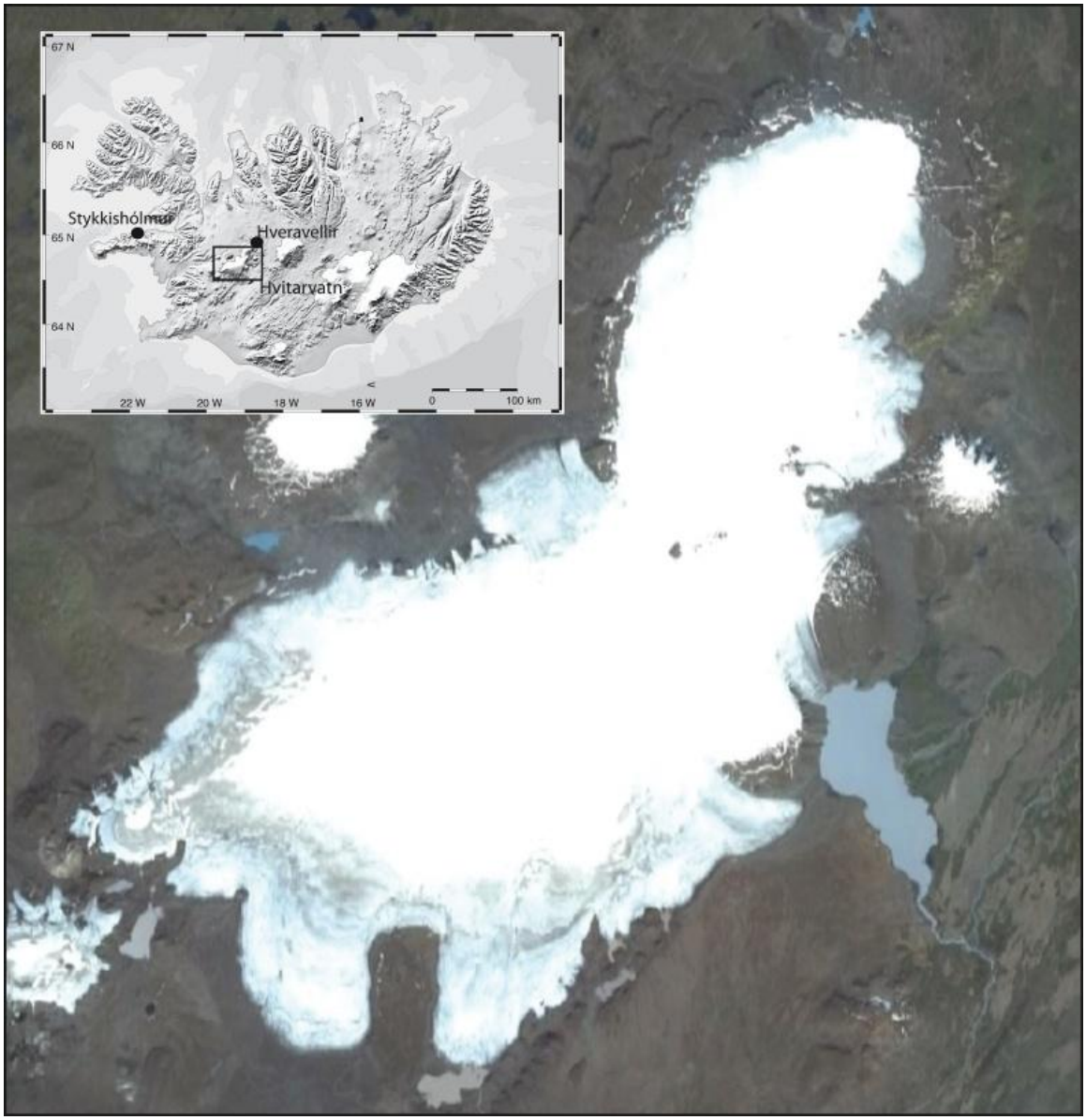

Figure 1 ***a)*** *The location of Hvítárvatn and the meteorological stations at Hveravellir and Stykkishólmur.* ***b)*** *Hvítárvatn is located on the eastern margin of Langjökull the second's largest glacier in Iceland (920 km²).*

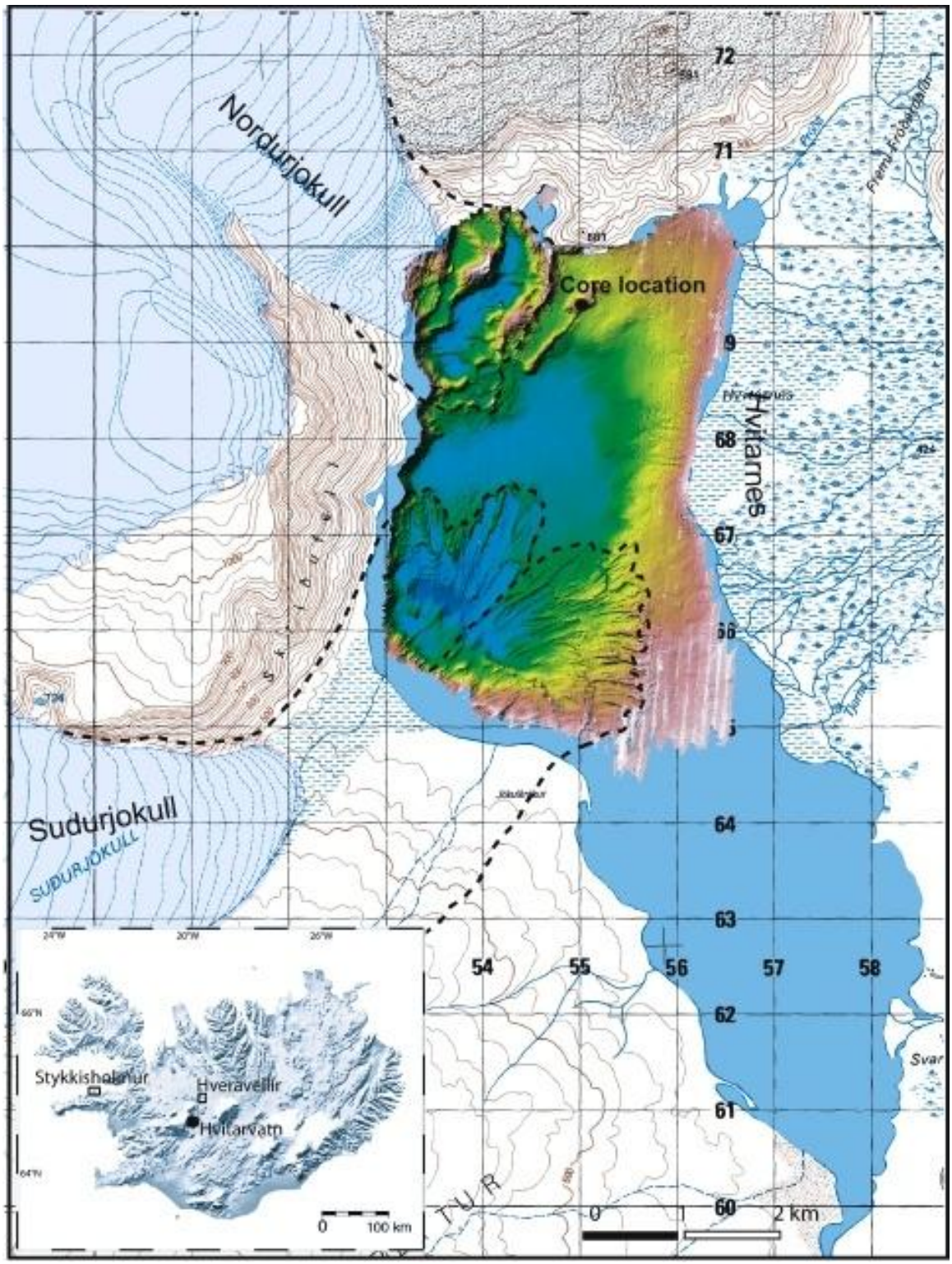

Figure 2 *Topographic map of Hvítárvatn and Langjökull. The ice margins of Norðurjökull and Suðurjökull are shown on the map along with their approximate LIA maximum limit. The location of the core under discussion is shown as black circle on the topographic map*

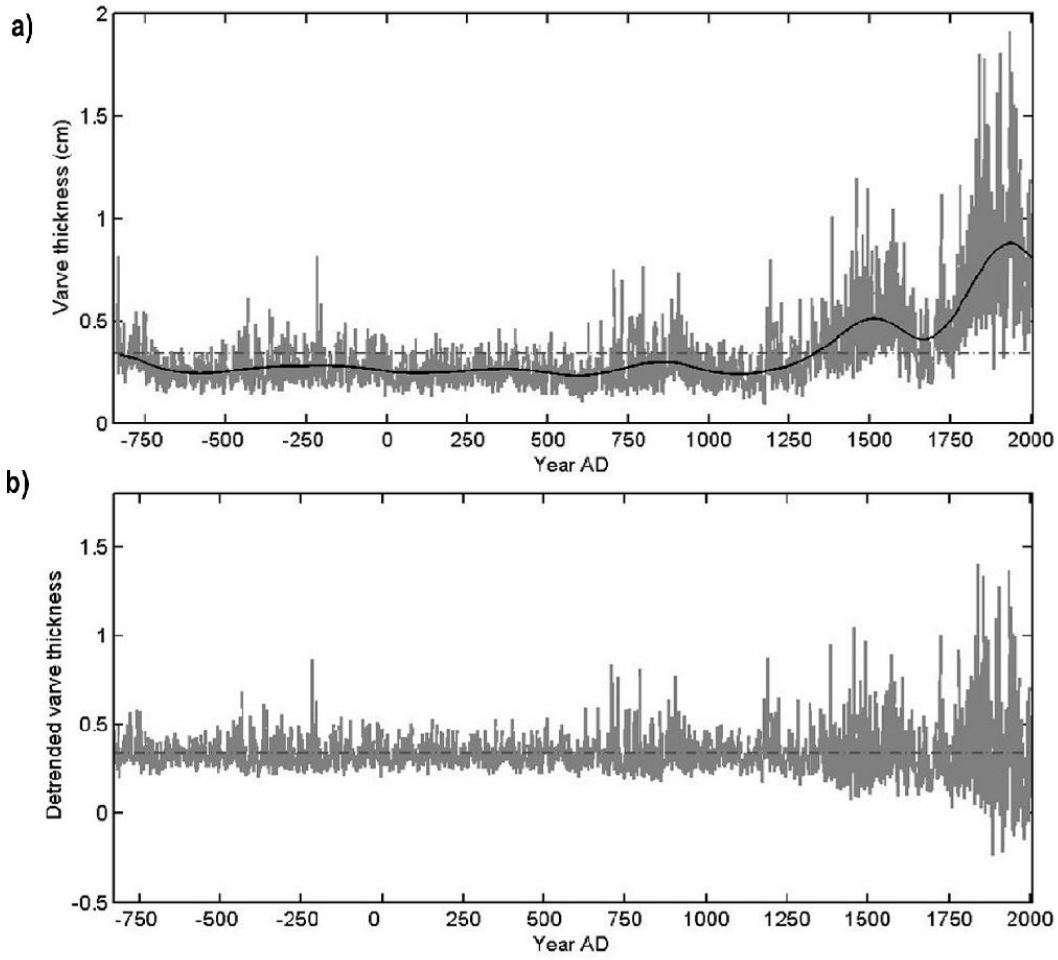

Figure 3 ***a)*** *The original raw varve thickness (grey line) with the mean value plotted with grey dotted line. A non-linear long term trend (black line); a composite of ~1000 year cycle and ~500 year cycle estimated with SSA, was filtered out prior to the spectral analysis****. b)*** *The detrended varve thickness record used in the spectral analysis. The mean value is indicated with grey dotted line.*

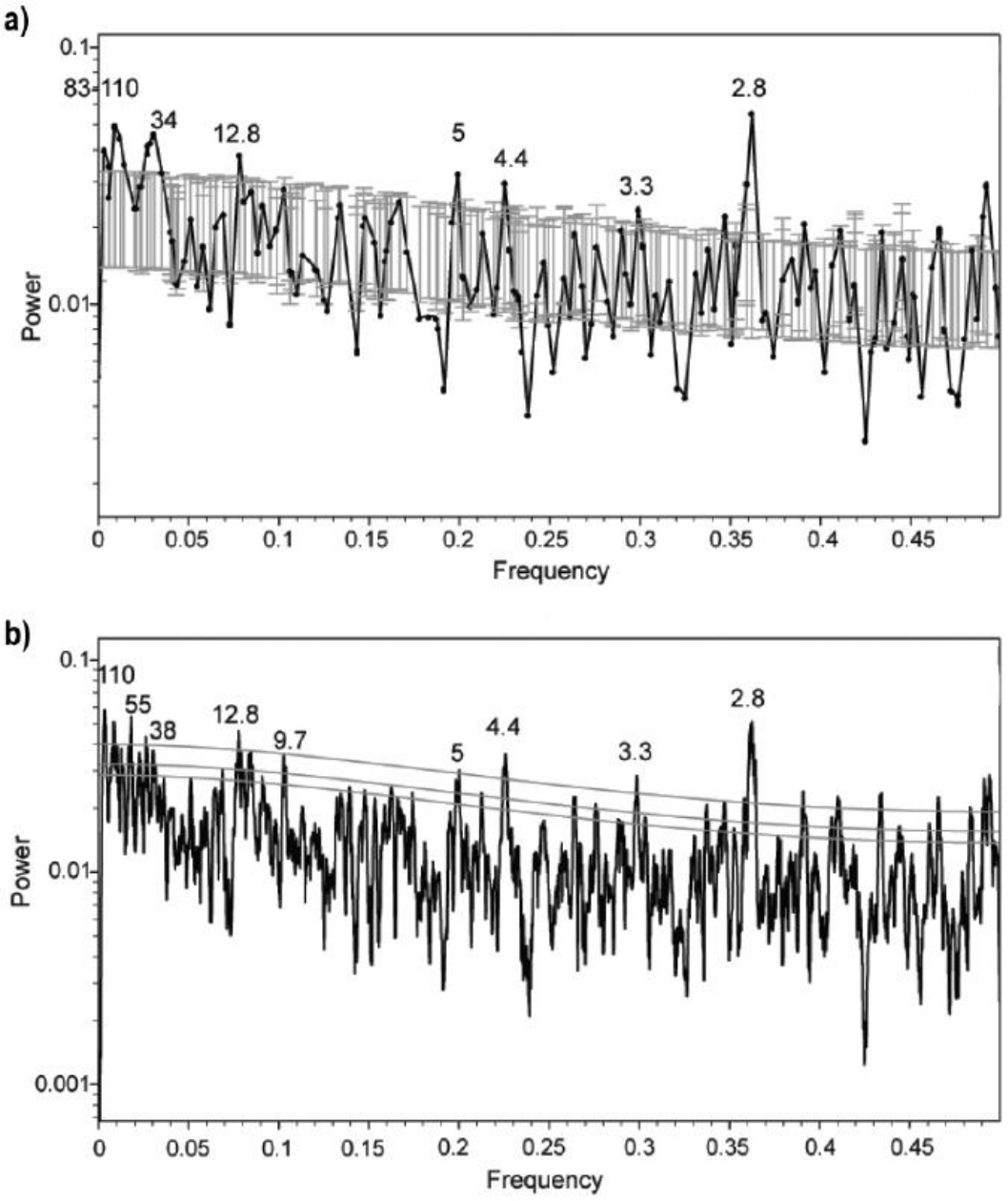

Figure 4 *Spectral analyses for the detrended varve thickness from Hvítárvatn.* ***a)*** *SSA spectrum (black line) with 95% confidence level (grey bars).* ***b)*** *MTM spectrum (black line) with 90, 95 and 99% significance levels (grey lines). The common spectral peaks in both methods are cycles of 110, 34, 12.8, 5, 4.4, 3.3 and 2.8 years. Additionally cycles of 55 and 9.7 years are indicated in the MTM spectrum.*

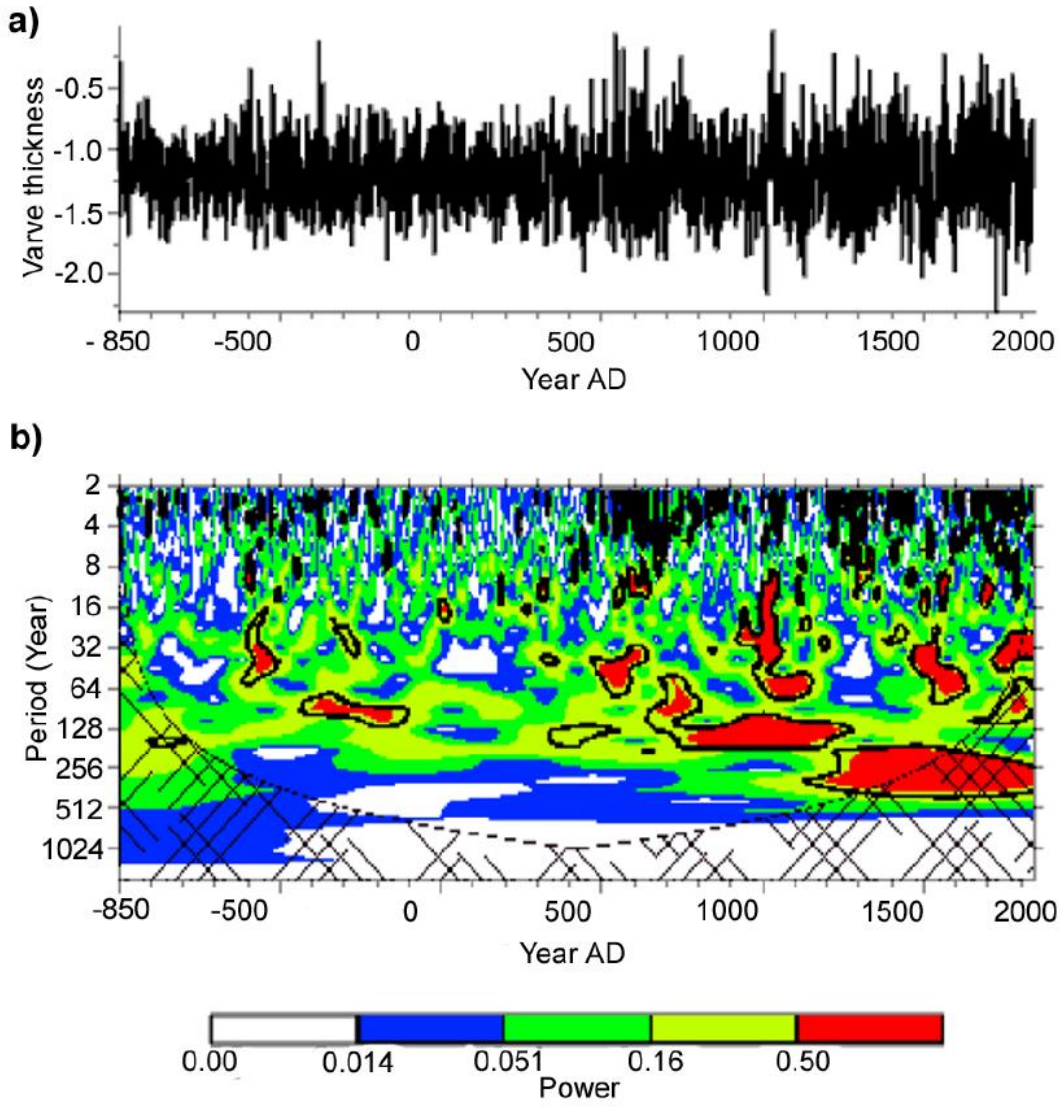

Figure 5 ***a)*** *The detrended varve thickness time series was log-transformed prior to the wavelet analysis in order to stabalize the variance.* ***b)*** *Wavelet power spectrum of the varve thickness using the Morlet wavelet. The black contour is the 10% significance level using a red noise background spectrum and the cross-hatched region is the cone of influence.*

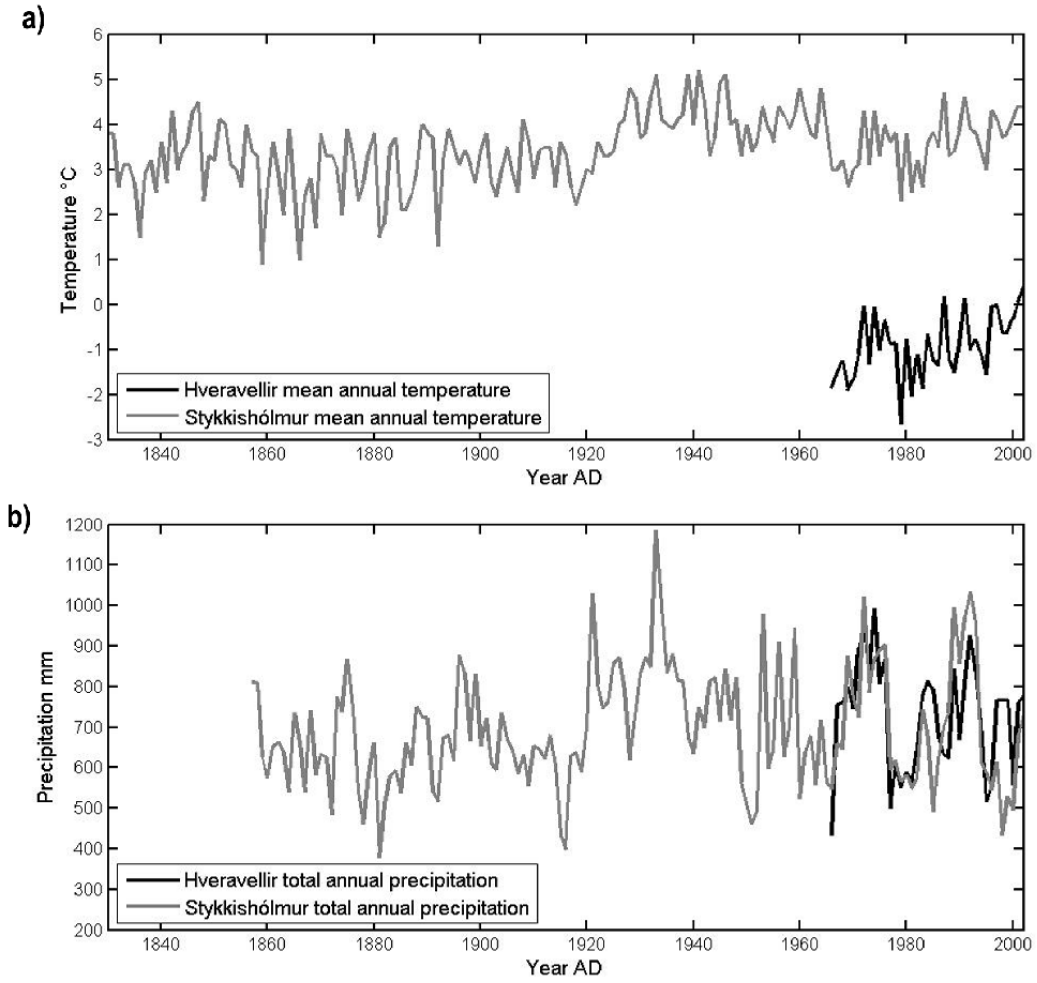

Figure 6 ***a)*** *The annual mean temperature from Stykkishólmur (2002 – 1830 AD) – grey line. The annual mean temperature from Hveravellir (2002 – 1966 AD) – black line. The correlation coefficient for the overlap period is 0.95; p <0.0001.* ***b)*** *The total annual precipitation from Stykkishólmur (2002 – 1857 AD) – grey line. The total annual precipitation from Hveravellir (2002 -1966 AD) – black line. The correlation coefficient for the overlap period is 0.66; p<0.0001. The climate records are from the Icelandic Meteorological Office (http://www.vedur.is/)*

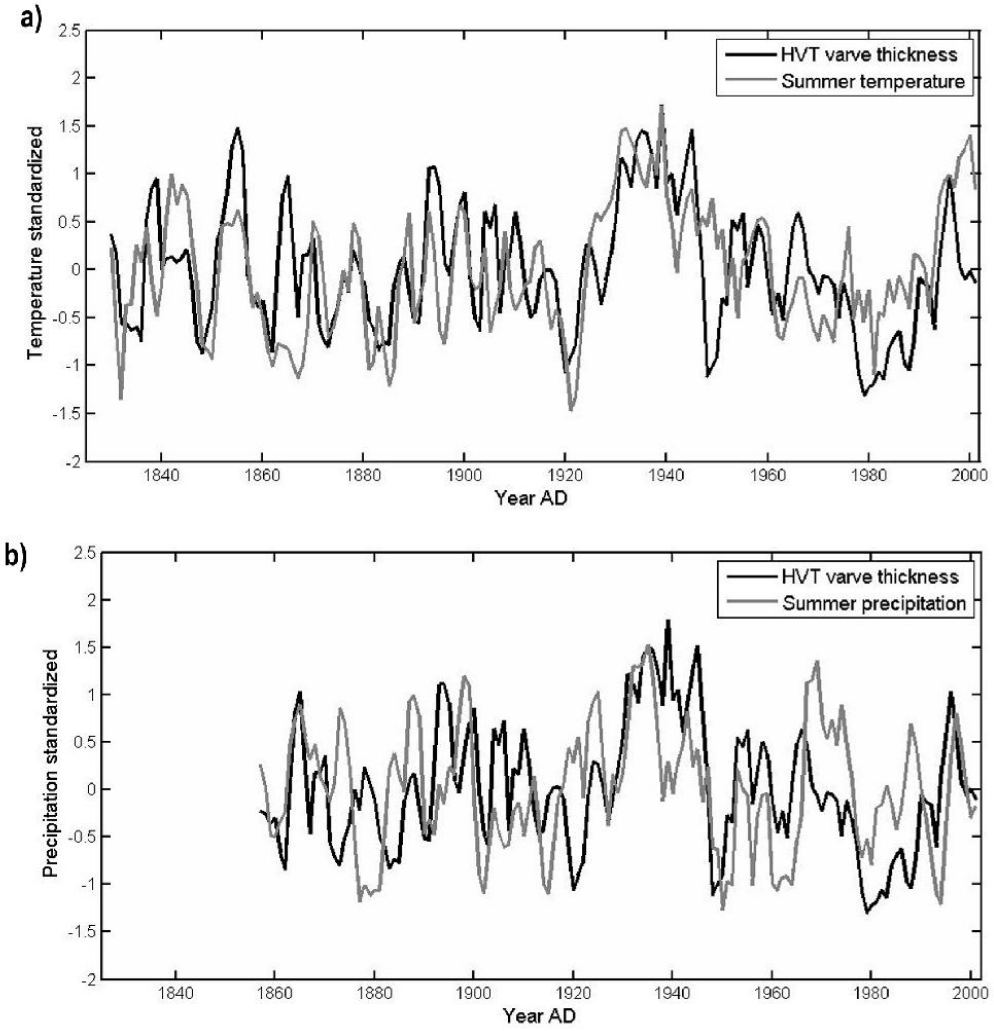

Figure 7 ***a)*** *HVT Varve thickness (grey line) compared with summer (mean values of June, July, August and September) temperature, a composite record of temperature records from Hveravellir and Stykkishólmur (black line).* ***b)*** *HVT Varve thickness (grey line) compared with total summer (June, July, August and September) precipitation, a composite record of precipitation from Hveravellir and Stykkishólmur. In both plots the values have been smoothed with 3 year moving average filter and the climatic parameters have been moved 1 lag forward.*

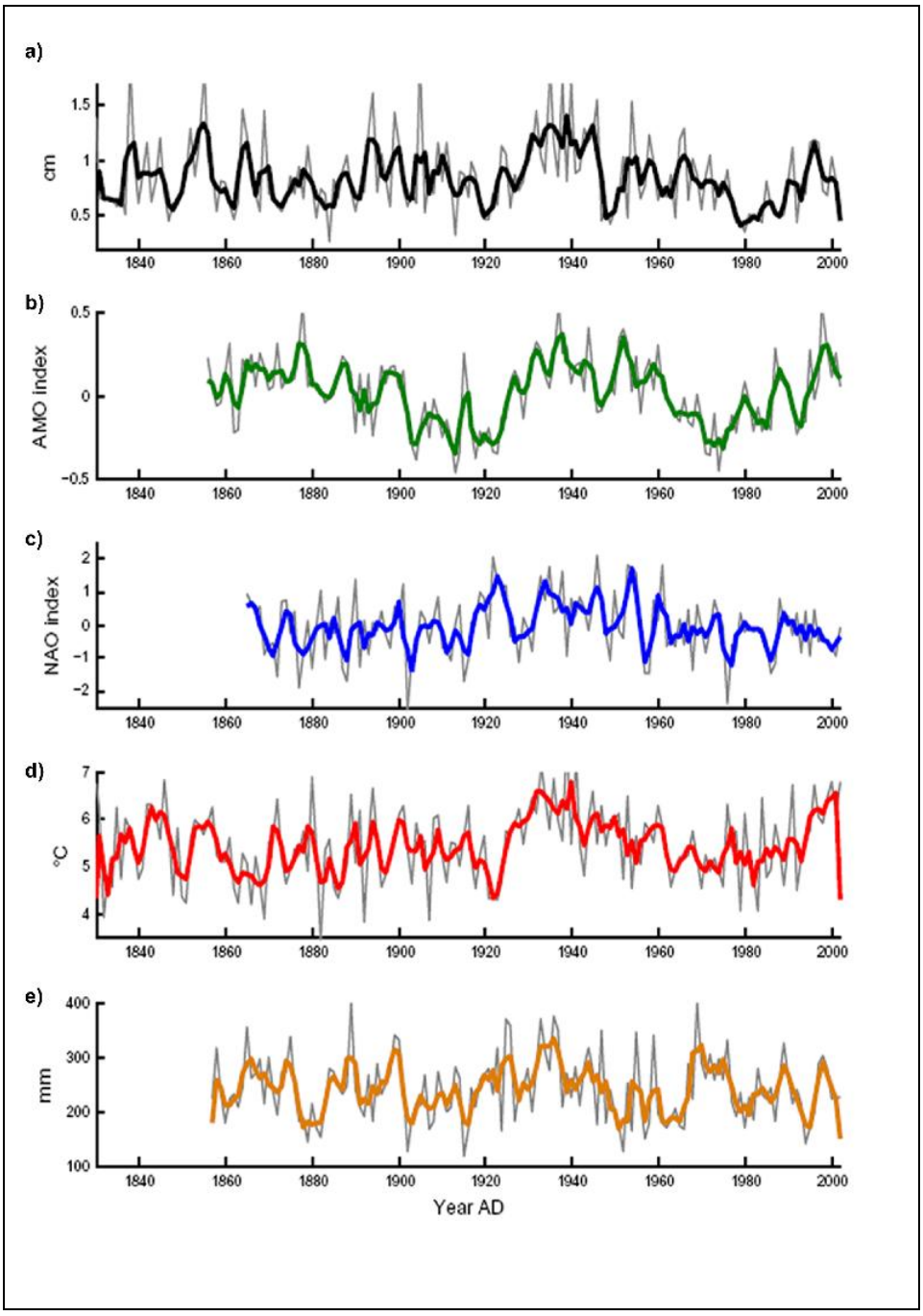

Figure 8 ***a)*** *The HVT varve thickness. Grey line shows raw data and the black line shows a 3 year moving average.* ***b)*** *The Summer AMO index (Einfield et al., 2001), the mean value of June, July, August and September. Grey line shows raw data and the green line shows a 3 year moving average.* ***c)*** *The Summer NAO index (Hurrell, 1995), the mean value of June, July, August and September. Grey line shows raw data and the blue line shows a 3 year moving average.* ***d)*** *The reconstructed summer temperature (mean value of June, July, August and September temp.), a composite record of temperature records from Hveravellir and Stykkishólmur. The grey line is raw data and the red line shows a 3 year moving average.* ***e)*** *The reconstructed summer precipitation (total precipitation in June, July, August and September), a composite record of temperature records from Hveravellir and Stykkishólmur. The grey line is raw data and the orange line shows a 3 year moving average.*

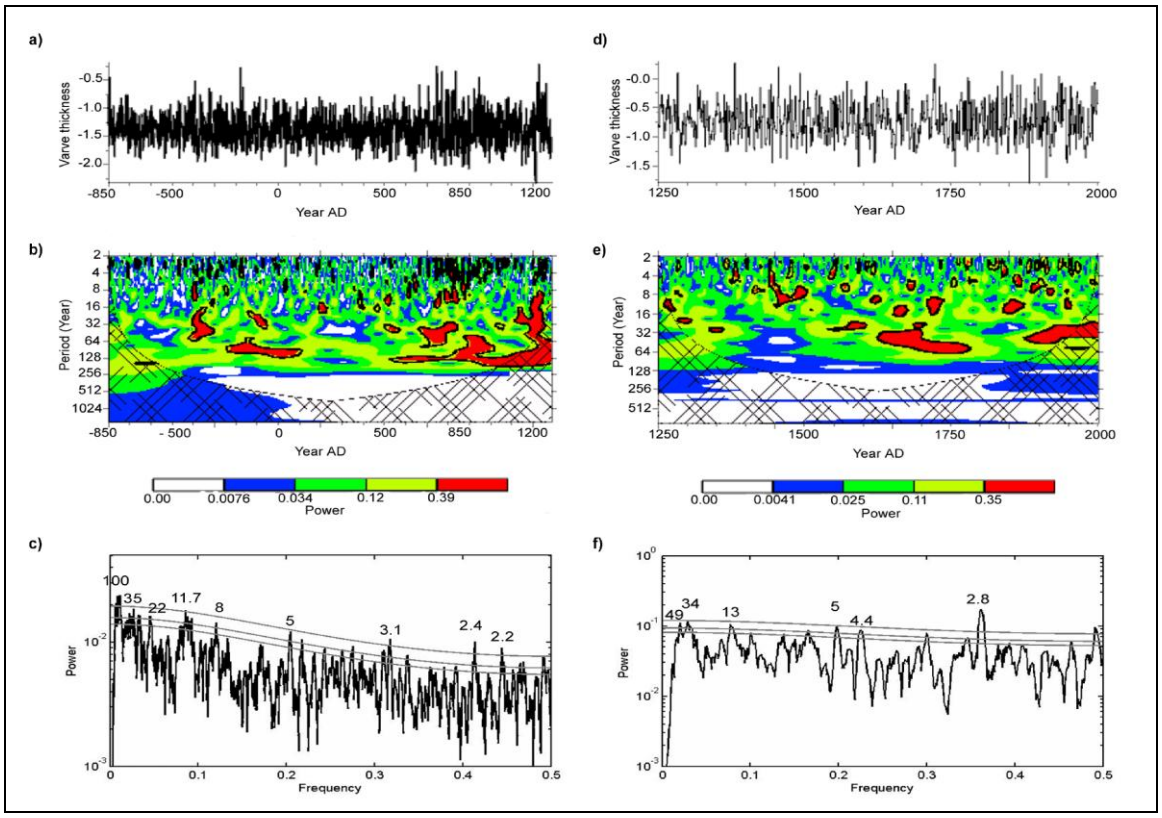

Figure 9 ***a)*** *The earlier time series; covers the more stable part (1250 AD – 830 BP). The data was detrended and log-transformed prior to the wavelet analysis.* ***b)*** *Wavelet spectrum for the Neoglaciation part. It was calculated using the Morlet wavelet. The black contour is the 10% significant level using a red noise backgroun spectrum and the cross-hatched region is the cone of influence.* ***c)*** *MTM power spectrum for the detrended Neoglaciation part (black lines), numbers of tapers were 7 and bandwidth 5. The grey lines show 90, 95 and 99% significant levels.* ***d)*** *The younger time series; Little Ice Age (LIA), covers the more unstable part (2002 – 1250 AD). The data were detrended and log-transformed prior to the wavelet analysis.* ***e)*** *Wavelet spectrum for the LIA portion. It was calculated using the Morlet wavelet. The black contour is the 10% significant level using a red noise background spectrum and the cross-hatched region is the cone of influence.* ***f)*** *MTM power spectrum for the detrended LIA part (black lines), number of tapers were 5 and bandwidth 3. The 90, 95 and 99% significant levels are shown with grey lines.*

Table 1 ***The upper part;*** *shows the correlation coefficient between the HVT varve thickness and estimated temperature record, composite record of temperature records from Hveravellir (2002 -1966 AD) and Stykkishólmur (1965 – 1830 AD).* ***The lower part;*** *shows the correlation coefficient between HVT varve thickness and estimated precipitation record, a composite record of precipitation record from Hveravellir (2002 – 1966 AD) and Stykkishólmur (1965 – 1857 AD). All records were smoothed with 3 year moving average filter. If $p < 0.05$; then the correlation is significant at a 95% significance level. The significant r-values are written in bold.*

HVT varve thickness vs. Hveravellir estimated temperature		
n = 173		
lag $_{\text{temperature}}$ +1		
	r	**p value**
Mean annual	**0,36**	<0,001
Mean winter (December ,January ,February, March)	0,11	0,153
Mean spring (April, May)	**0,36**	<0,001
Mean summer (June, July, August, September)	**0,54**	<0,001
Mean fall (October, November)	**0,23**	0,002
Mean (May, June, July, August, September)	**0,53**	<0,001
Mean(July, August, September)	**0,51**	<0,001

HVT varve thickness vs. Hveravellir estimated precipitation		
n = 146		
lag $_{\text{precipitation}}$ +1		
	r	**p value**
Total annual	**0,34**	<0,001
Total winter (Dec, Jan, Feb, March)	0,12	0,137
Total spring (April, May)	**0,28**	0,001
Total Summer (June, July, August, Sept)	**0,36**	<0,001
Total fall (October, November)	**0,27**	0,001
Total (May, June, July, August, Sept)	**0,40**	<0,001
Total (July, August, September)	**0,45**	<0,001

Table 2 *The correlation coefficient between NAO summer index and several parameters shown in the left part. The correlation coefficient between the AMO summer index and several parameters are shown in the right part. The significant r-values are written in bold.*

	NAO (summer)			AMO (summer)		
	r	**p-value**	**n**	**r**	**p**	**n**
HVT varve thickness	**0,28**	0,001	138	**0,34**	<0,001	147
Temperature (summer)	0,04	0,672	138	**0,45**	<0,001	147
Precipitation (summer)	**0,38**	<0,001	138	0,10	0,213	146
NAO (summer)	-	-	138	0,11	0,190	138
AMO (summer)	0,11	0,190	138	-	-	147

If $p < 0.05$; then the correlation is significant at a 95% significance level

All the records have been smoothed with 3 year moving average

The instrumental records have been moved 1 year ahead of the HVT varve thickness